https://doi.org/10.5194/essd-2020-308
Preprint. Discussion started: 15 April 2021

Open Access Earth System Science Data Discussions

Climate-Biogeochemistry Interactions in the Tropical Ocean: Data collection and legacy

Gerd Krahmann[1], Damian L. Arévalo-Martínez[1], Andrew W. Dale[1], Marcus Dengler[1], Anja Engel[1], Nicolaas Glock[1], Patricia Grasse[1,2], Johannes Hahn[3,1], Helena Hauss[1], Mark J. Hopwood[1], Rainer Kiko[1,4], Alexandra Loginova[1,5], Carolin R. Löscher[6], Marie Maßmig[1], Alexandra-Sophie Roy[7], Renato Salvatteci[8,9], Stefan Sommer[1], Toste Tanhua[1], Hela Mehrtens[1]

[1]GEOMAR, Helmholtz Centre for Ocean Research Kiel, Kiel, 24148, Germany
[2]German Centre for Integrative Biodiversity Research (iDiv) Halle-Jena-Leipzig, Leipzig, 04103, Germany
[3]Federal Maritime and Hydrographic Agency Bernhard-Nocht-Str. 78, 20359 Hamburg, Germany
[4]Laboratoire d'Océanographie de Villefranche-sur-Mer, 06320, France
[5]Institute of Oceanology of Polish Academy of Sciences, Powstańców Warszawy 55, 81-712 Sopot, Poland
[6]Nordcee, Department of Biology and DIAS, University of Southern Denmark, 5230 Odense M, Denmark
[7]Genomic Microbiology, Institute of Microbiology, Kiel University, Kiel, 24118, Germany
[8]Institute of Geosciences, Kiel University, Kiel, 24118, Germany
[9]Center for Ocean and Society, Kiel University, Kiel, 24118, Germany

Correspondence to: Gerd Krahmann (gkrahmann@geomar.de)

Abstract. From 2008 through 2019, a comprehensive research project, *SFB 754, Climate - Biogeochemistry Interactions in the Tropical Ocean*, was funded by the German Research Foundation to investigate the climate-biogeochemistry interactions in the tropical ocean with a particular emphasis on the processes determining the oxygen distribution. During three 4-year long funding phases, a consortium of more than 150 scientists conducted or participated in 34 major research cruises and collected a wealth of physical, biological, chemical, and meteorological data. A common data policy agreed upon at the initiation of the project provided the basis for the open publication of all data. Here we provide an inventory of this unique data set and briefly summarize the various data acquisition and processing methods used.

https://doi.org/10.5194/essd-2020-308
Preprint. Discussion started: 15 April 2021

1 Introduction

The distribution of oxygen in the ocean interior is controlled by an intimate interplay of physics and biogeochemistry. Circulation and mixing transport oxygen from the near-surface where it is produced by photosynthesis and exchanged with the atmosphere into the ocean interior. Oxygen consumption occurs throughout the ocean and is essentially driven by bacterial respiration of organic matter. Both the supply and consumption of oxygen are sensitive to climate change in ways that are not fully understood. A central objective of the Collaborative Research Center 754 (Sonderforschungsbereich SFB 754, Climate - Biogeochemistry Interactions in the Tropical Ocean) was to better understand the observed changes in ocean oxygen distribution (see Figure 1) and thoroughly investigate the climate-biogeochemistry system in the tropical Atlantic and Pacific Oceans. The program was financed from 2008 through 2019 by the German Research Foundation (DFG).

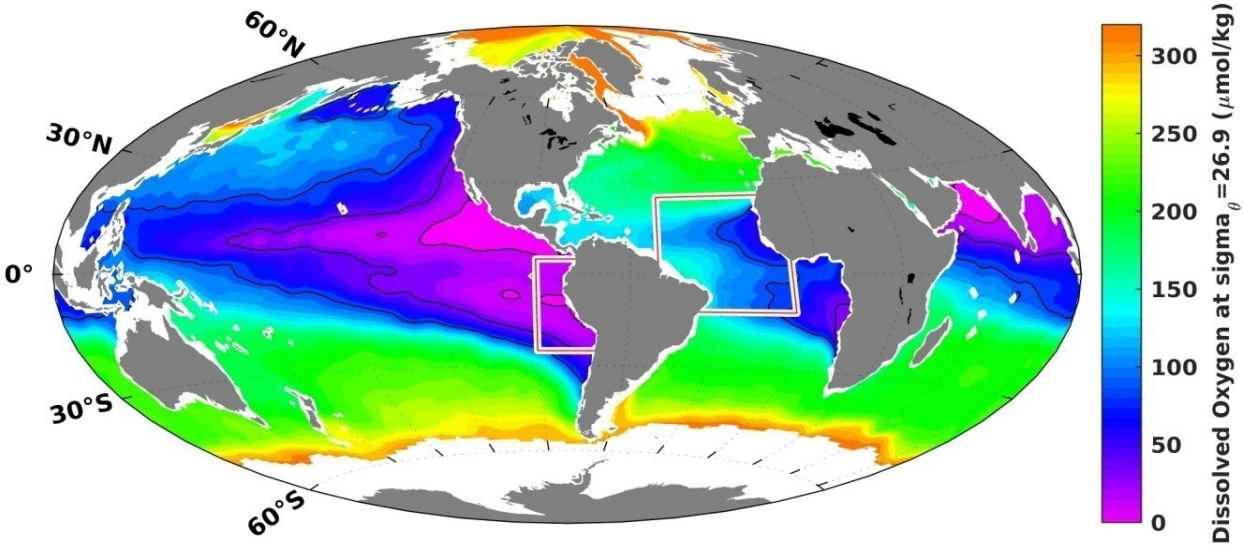

https://doi.org/10.5194/essd-2020-308
Preprint. Discussion started: 15 April 2021

Figure 1: The two working areas of the SFB 754 overlaid on the climatological content of dissolved oxygen on the potential density surface sigma$_\theta$ 26.9 (between 200 and 500 m depth in tropical regions). The map is based on data from the World Ocean Atlas 2018 (Garcia et al., 2018).

Addressing the SFB 754 goals required a highly multi-disciplinary approach. The SFB 754 built upon the wide-ranging marine expertise available at the GEOMAR Helmholtz Centre for Ocean Research Kiel and Kiel University, both in Kiel, Germany. Biological, chemical and physical oceanography, sediment biogeochemistry, marine ecology, molecular microbiology, paleoceanography, geology, as well as climate and biogeochemical modelling all contributed to the project. The SFB 754 was organised in 18 highly interdisciplinary science sub-projects striving to answer the key questions of the project. An outreach sub-project complemented the scientific sub-projects with programs for pupils and the general public. A dedicated central data management team was hosted by the GEOMAR data management and supported and supervised the curation and publication of all data collected by the SFB 754. The aim of this article is to describe and list the published observational data sets collected by the SFB 754 for easy access and find-ability.

2 Observational and experimental program

During the 12-year life-cycle the SFB 754 conducted or participated in a total of 34 research cruises on large research vessels (see Table 1 and Figures 2 and 3). Data from these cruises constitutes the bulk of the SFB 754 data. The three 4-year long phases allowed for the development and adaptation of the observational and experimental program. Questions arising from the data already collected were incorporated into new sub-projects for the subsequent project phases.

Table 1: Cruises on large research vessels in chronological order.

Cruise-id	Vessel	Start	End	Expocode	Cruise Report DOI	Main Funding
ATA_ IFMGEOMAR_ 4	N/O '*Atalante*	2008-02-23 Mindelo/Cape Verde	2008-03-15 Mindelo/Cape Verde	35A320080223	https://doi.org/10.3289/ifm-geomar_rep_19_2008	SFB 754; NORDATLANTIK

https://doi.org/10.5194/essd-2020-308
Preprint. Discussion started: 15 April 2021

MSM08/1	FS *Maria S. Merian*	2008-04-18 Mindelo/Cape Verde	2008-05-03 Mindelo/Cape Verde	06M220080420	https://doi.org/10.2312/cr_msm08	SFB 754
M77/1	FS *Meteor*	2008-10-22 Talcahuano/Chile	2008-11-21 Callao/Peru	06M320081022	https://doi.org/10.2312/cr_m77	SFB 754
MSM10/1	FS *Maria S. Merian*	2008-11-01 Ponta Delgada/Portugal	2008-12-06 Mindelo/Cape Verde	06M220081031	https://doi.org/10.2312/cr_msm10_1	SFB 754
M77/2	FS *Meteor*	2008-11-24 Callao/Peru	2008-12-22 Guayaquil/Ecuador	06M320081124	https://doi.org/10.2312/cr_m77	SFB 754
M77/3	FS *Meteor*	2008-12-27 Guayaquil/Ecuador	2009-01-23 Callao/Peru	06M320081227	https://doi.org/10.2312/cr_m77	SFB 754
M77/4	FS *Meteor*	2009-01-27 Callao/Peru	2009-02-18 Cristobal/Panama	06M320090127	https://doi.org/10.2312/cr_m77	SFB 754
M80/1	FS *Meteor*	2009-10-26 Mindelo/Cape Verde	2009-11-23 Mindelo/Cape Verde	06M320091026	https://doi.org/10.2312/cr_m80_1	Future Ocean II; SFB 754; NORDATLANTIK
M80/2	FS *Meteor*	2009-11-26 Mindelo/Cape Verde	2009-12-23 Dakar/Senegal	06M320091126	https://doi.org/10.2312/cr_m80_2	SFB 754
M83/1	FS *Meteor*	2010-10-17 Las Palmas/Spain	2010-11-13 Mindelo/Cape Verde	06M320101017	https://doi.org/10.2312/cr_m83_1	Future Ocean II; SFB 754
MSM17/4	FS *Maria S. Merian*	2011-05-11 Dakar/Senegal	2011-04-12 Las Palmas/Spain	06M220110511	https://doi.org/10.2312/cr_msm17_4	SFB 754
MSM18/2	FS *Maria S. Merian*	2011-05-11 Mindelo/Cape Verde	2011-06-19 Mindelo/Cape Verde	06M220110511	https://doi.org/10.2312/cr_msm18_2	NORDATLANTIK; SOPRAN; SFB 754
MSM18/3	FS *Maria S. Merian*	2011-06-22 Mindelo /Cape Verde	2011-07-21 Libreville/Gabon	06M220110622	https://doi.org/10.2312/cr_msm18_3	SOPRAN; SFB 754
MSM22	FS *Maria S. Merian*	2012-10-24 Mindelo/Cape Verde	2012-11-23 Mindelo/Cape Verde	06M220121024	https://doi.org/10.2312/cr_msm22	SFB 754; NORDATLANTIK; RACE; SOPRAN; CARBOCHANGE
M90	FS *Meteor*	2012-10-28 Cristobal/Panama	2012-11-28 Callao/Peru	06M320121028	https://doi.org/10.2312/cr_m90	SFB 754

https://doi.org/10.5194/essd-2020-308
Preprint. Discussion started: 15 April 2021

MSM23	FS *Maria S. Merian*	2012-11-26 Mindelo/Cape Verde	2012-12-20 Walvis Bay/Namibia	06M220121126	https://doi.org/10.2312/cr_msm23	SFB 754
M91	FS *Meteor*	2012-12-01 Callao/Peru	2012-12-26 Callao/Peru	06M320121201	https://doi.org/10.2312/cr_m91	SOPRAN; SFB 754
M92	FS *Meteor*	2013-01-05 Callao/Peru	2013-02-03 Callao/Peru	06M320130105	https://doi.org/10.2312/cr_m92	SFB 754
M93	FS *Meteor*	2013-02-06 Callao/Peru	2013-03-10 Cristobal/Panama	06M320130206	https://www.ldf.uni-hamburg.de/meteor/wochenberichte/wochenberichte-meteor/m90-m93/m93-scr.pdf Short cruise report only	SFB 754
M96	FS *Meteor*	2013/04/28 Pointe A Pierre/Trinidad and Tobago	2013/05/23 Mindelo/Cape Verde	06M320130428	https://doi.org/10.2312/cr_m96	SFB 754
M97	FS *Meteor*	2013-05-25 Mindelo/Cape Verde	2013-06-28 Fortaleza/Brazil	06M320130525	https://doi.org/10.2312/cr_m97	SFB 754
M105	FS *Meteor*	2014-03-17 Mindelo/Cape Verde	2014-04-16 Mindelo/Cape Verde	06M320140317	https://doi.org/10.2312/cr_m105	SFB 754; CARBOCHANGE; SOPRAN
M106	FS *Meteor*	2014-04-19 Mindelo/Cape Verde	2014-05-26 Fortaleza/Brazil	06M320140419	https://doi.org/10.2312/cr_m106	SFB 754; RACE
M107	FS *Meteor*	2014-05-29 Fortaleza/Brazil	2014-07-03 Las Palmas/Spain	06M320140529	https://doi.org/10.2312/cr_m107	SFB 754
M116/1	FS *Meteor*	2015-05-01 Pointe-à-Pitre/Guadeloupe	2015-06-03 Mindelo/Cape Verde	06M320150501	https://doi.org/10.2312/cr_m116_1	SFB 754
SO241	FS *Sonne*	2015-06-23 Manzanillo/Mexico	2015-07-24 Guayaquil/Ecuador	06SN20150623	https://doi.org/10.3289/CR_S241	MAKS
M119	FS *Meteor*	2015-09-08 Mindelo/Cape Verde	2015-10-13 Recife/Brazil	06M320150908	https://doi.org/10.2312/cr_m119	SFB 754; RACE
SO243	FS *Sonne*	2015-10-05 Guayaquil/Ecuador	2015-10-22 Antofagasta/Chile	06SN20151005	https://doi.org/10.3289/CR_SO243	ASTRA-OMZ
M130	FS *Meteor*	2016-08-28 Mindelo/Cape Verde	2016-10-03 Recife/Brazil	06M320160828	https://doi.org/10.3289/CR_M130	SFB 754; RACE

https://doi.org/10.5194/essd-2020-308
Preprint. Discussion started: 15 April 2021

M135	FS *Meteor*	2017-03-02 Valparaiso/Chile	2017-04-08 Callao/Peru	06M320170302	https://doi.org/10.2312/cr_m135	SFB 754
M136	FS *Meteor*	2017-04-11 Callao/Peru	2017-05-03 Callao/Peru	06M320170411	https://doi.org/10.3289/CR_M136	SFB 754
M137	FS *Meteor*	2017-05-06 Callao/Peru	2017-05-29 Callao/Peru	06M320170506	https://doi.org/10.2312/cr_m137	SFB 754
M138	FS *Meteor*	2017-06-01 Callao/Peru	2017-07-03 Bahia De Las Minas/Panama	06M320170601	https://doi.org/10.2312/cr_m138	SFB 754
M145	FS *Meteor*	2018-02-15 Mindelo/Cape Verde	2018-03-13 Recife/Brazil	06M320180215	https://doi.org/10.2312/cr_m145	SFB 754; RACE

https://doi.org/10.5194/essd-2020-308
Preprint. Discussion started: 15 April 2021

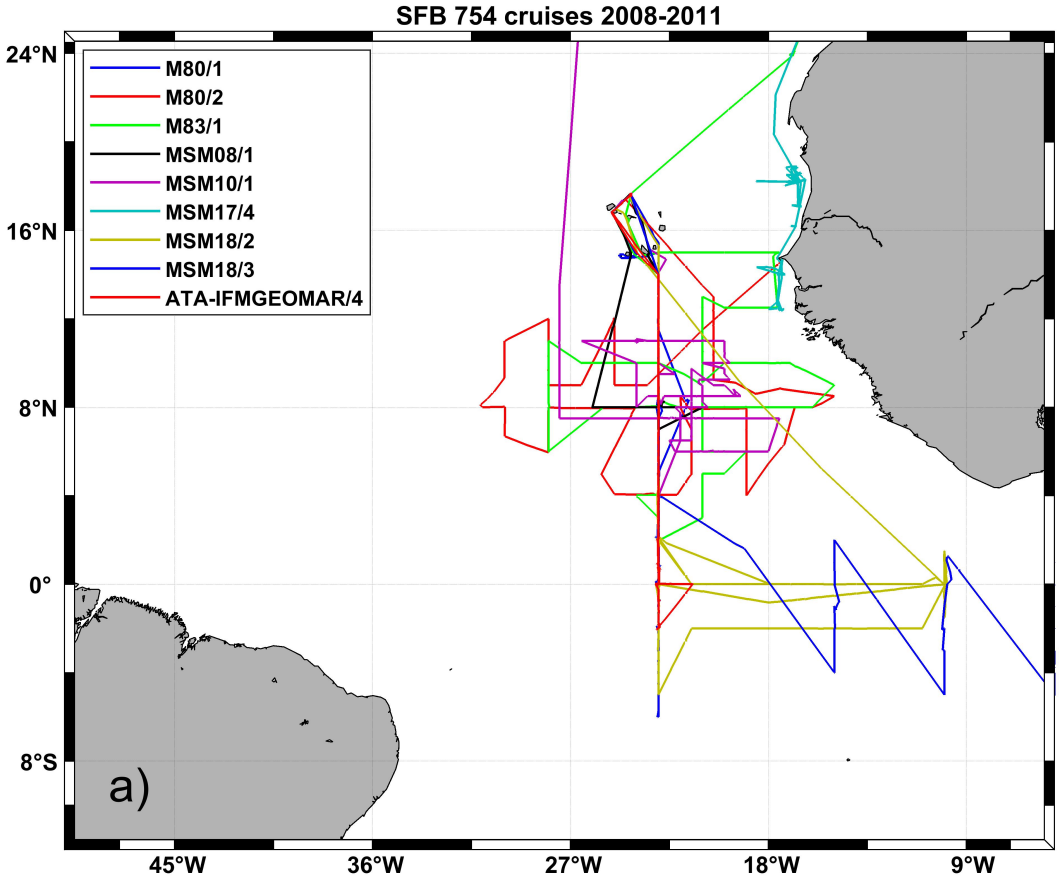

https://doi.org/10.5194/essd-2020-308
Preprint. Discussion started: 15 April 2021

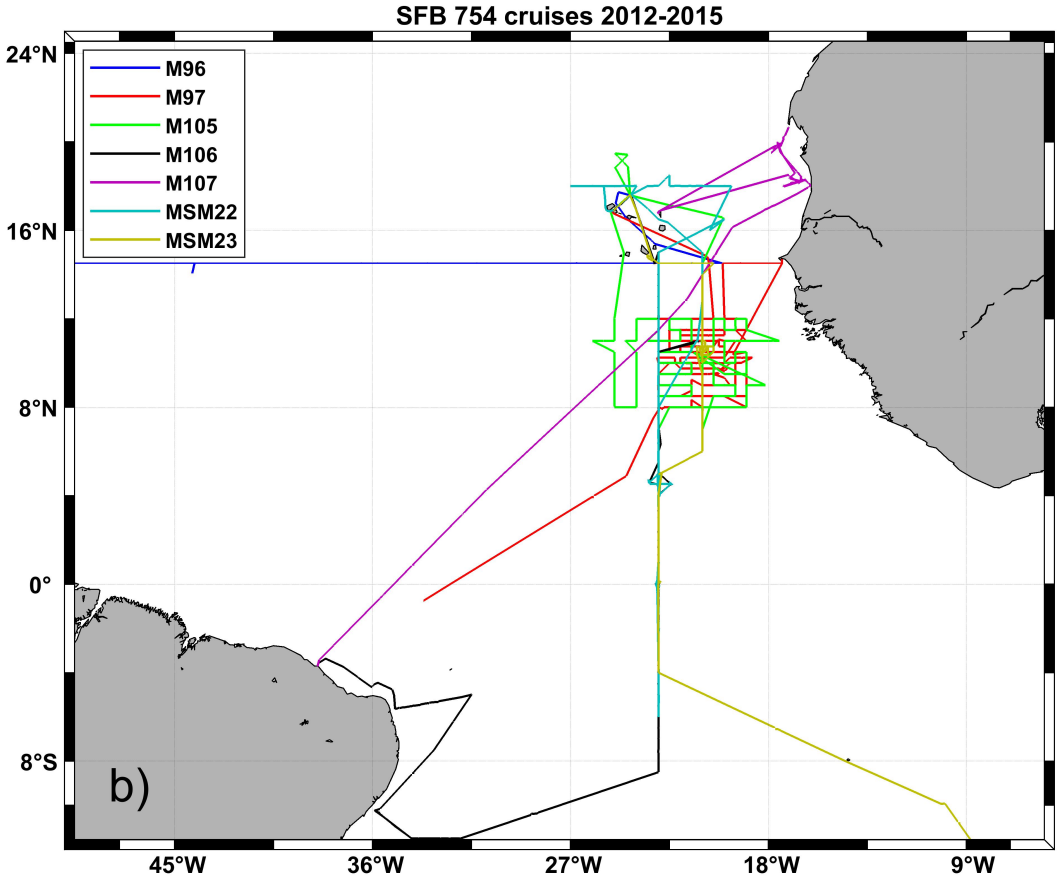

https://doi.org/10.5194/essd-2020-308
Preprint. Discussion started: 15 April 2021

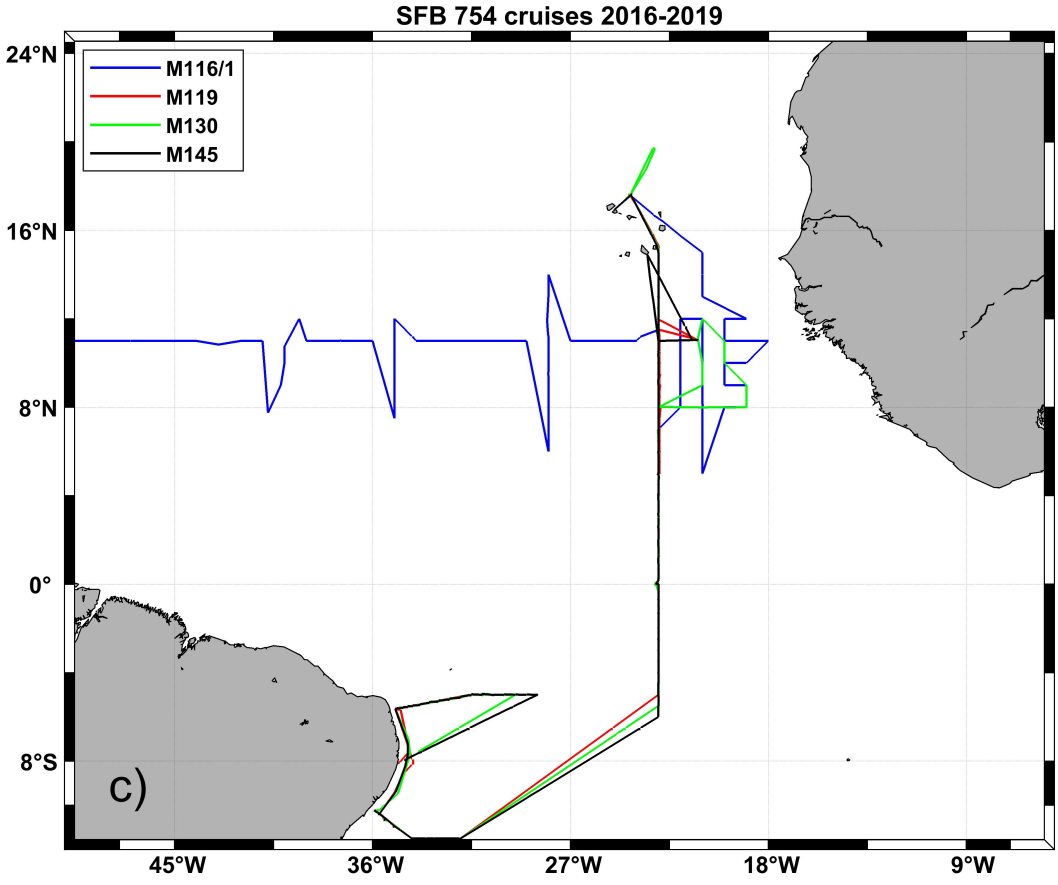

Figure 2: Cruise tracks of 20 SFB 754 cruises in the Atlantic Ocean. The three panels show the cruises for the respective funding periods of the project (a: 2008-2011, b: 2012-2015, c: 2016-2019).

https://doi.org/10.5194/essd-2020-308
Preprint. Discussion started: 15 April 2021

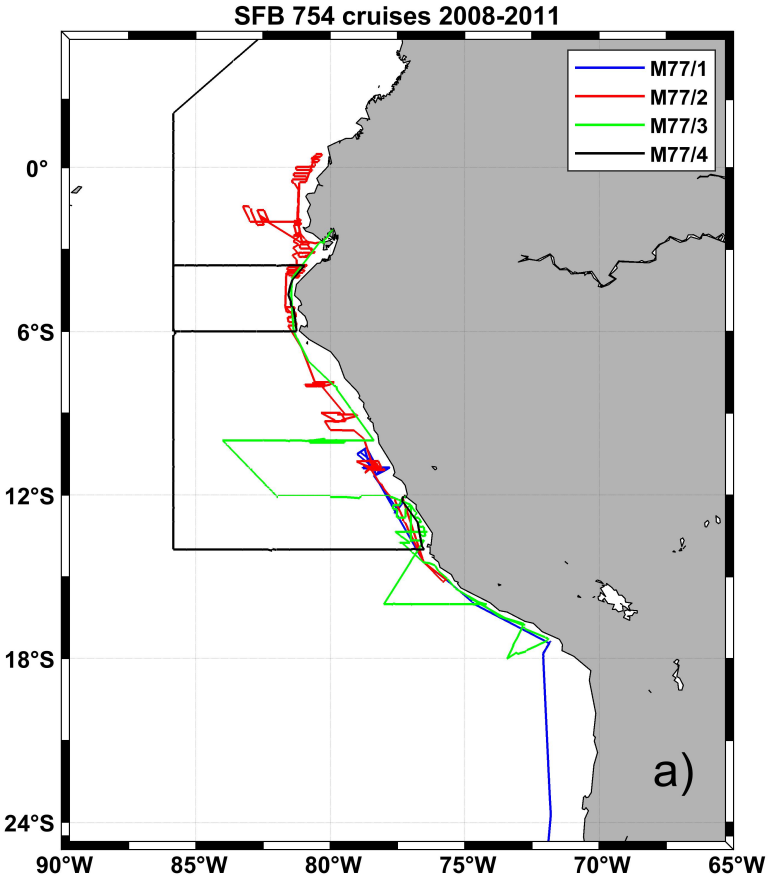

https://doi.org/10.5194/essd-2020-308
Preprint. Discussion started: 15 April 2021

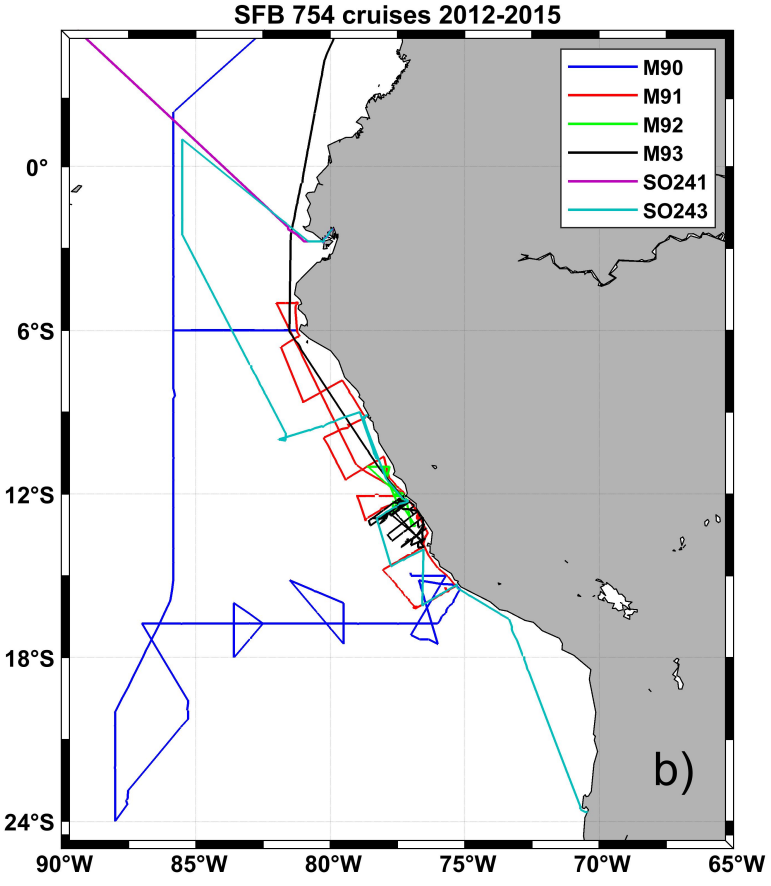

https://doi.org/10.5194/essd-2020-308
Preprint. Discussion started: 15 April 2021

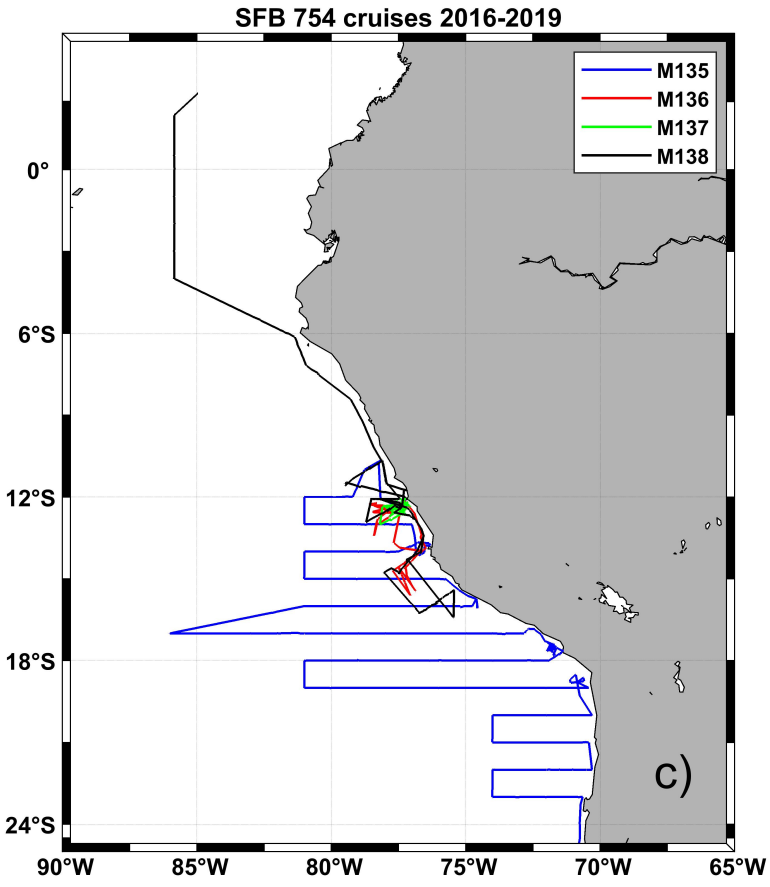

Figure 3: Cruise tracks of 14 SFB 754 cruises in the Pacific. The three panels show the cruises for the respective funding periods of the project (a: 2008-2011, b: 2012-2015, c: 2016-2019).

3 Data management

One of the first steps after the inception of the SFB 754 was the development and implementation of a common data policy (https://oceanrep.geomar.de/47369). Binding for all scientists of the SFB 754, it regulated how fully processed data sets should be curated, stored, distributed, and finally published, as well as the latency of this process. This data policy and its strict application is one of the reasons for the success of the SFB 754 with 421 peer reviewed publications at the time of writing.

https://doi.org/10.5194/essd-2020-308
Preprint. Discussion started: 15 April 2021

The data management was based on two pillars: The data was stored for, and distributed among, the scientists of the SFB 754 within the Ocean Science Information System (OSIS, https://www.sfb754.de/sfb754-osis) of GEOMAR. OSIS allows for the storage of different versions of the data set from preliminary and raw data shortly after collection, over calibrated data to the final data ready for publication. In the final step the data was published and made freely available at the World Data Center PANGAEA (https://www.pangaea.de) or at other more specific data centers.

Because of the diverse scientific fields and measurements involved, the rules of the data policy were quite generic. At the same time, an important goal was to ensure the timely exchange of data between the various research groups within the SFB 754. Within 3 months after data collection, meta-data for the measurements had to be entered into OSIS, and after 6 months initial versions had to be uploaded. The final publication of the data on PANGAEA was due 3 years after collection leaving sufficient time for analyses by members of the SFB 754. To support the adherence to the rules automatic reminders were sent by OSIS to the scientists responsible for the data sets. More than 1000 data sets have to date been published on PANGAEA (see https://www.pangaea.de/?q=sfb754 for a complete and up-to-date listing), while a small number is still being processed and will be published in the near future. For easier accessibility, the data from the different scientific fields using different methods and instruments have been separated into data collections at PANGAEA (see Table 2). Some of the data sets have been published elsewhere on more specialized databases. These are explicitly mentioned in the text below.

Table 2: Dataset collections at PANGAEA related to the descriptive sections. Abbreviations used are CTDO: Conductivity-Temperature-Depth - Oxygen, ADCP: Acoustic Doppler Current Profiler, UCTD: Underway Conductivity-Temperature-Depth, BIGO: Biogeochemical Observatory.

Section	DOI	Supplementary Table	Reference
4.1.1 CTDO	https://doi.org/10.1594/PANGAEA.926065	S1	Krahmann and Mehrtens (2021a)
4.1.2 Lowered ADCP	https://doi.org/10.1594/PANGAEA.926517	S2	Krahmann and Mehrtens (2021b)
4.1.3 Moored Instruments	https://doi.org/10.1594/PANGAEA.926545	S3	Hahn et al. (2021)
4.1.4 Salinometry	https://doi.org/10.1594/PANGAEA.926065	S1	Krahmann and Mehrtens (2021a)
4.1.5 Autonomous Gliders	https://doi.org/10.1594/PANGAEA.926547	S4	Krahmann and Mehrtens (2021c)

https://doi.org/10.5194/essd-2020-308
Preprint. Discussion started: 15 April 2021

4.1.6 Ocean Turbulence	https://doi.org/10.1594/PANGAEA.926518	S5	Dengler and Mehrtens (2021)
4.1.7 Shipboard ADCP	https://doi.org/10.1594/PANGAEA.926521	S6	Krahmann and Mehrtens (2021d)
4.1.8 UCTD and Rapidcast	https://doi.org/10.1594/PANGAEA.926529	S7	Krahmann and Mehrtens (2021e)
4.1.9 Thermosalinograph	https://doi.org/10.1594/PANGAEA.926530	S8	Krahmann and Mehrtens (2021f)
4.1.10 Argo Floats	https://doi.org/10.1594/PANGAEA.926544	S9	Krahmann and Mehrtens (2021g)
4.2.1 Water Sample Oxygen 4.2.2 Nutrients 4.2.3 Transient Tracers 4.2.4 Nitrous Oxide	https://doi.org/10.1594/PANGAEA.926609	S10	Tanhua and Mehrtens (2021)
4.2.5 Dissolved Silicate, Nitrate, and Nitrite Isotopes 4.2.6 Radiogenic Isotopes	https://doi.org/10.1594/PANGAEA.926610	S11 S12	Grasse and Mehrtens (2021)
4.2.7 Underway Trace Gases	https://doi.org/10.1594/PANGAEA.926611	S13	Arevalo-Martinez and Mehrtens (2021)
4.2.8 Trace chemical species	https://doi.org/10.1594/PANGAEA.928126	S14	Croot et al. (2021)
4.3.1 Particulate Organic Matter and Pigments	https://doi.org/10.1594/PANGAEA.926612	S15	Engel and Mehrtens (2021)
4.3.2 Dissolved Organic Matter, Cell Abundance, Extracellular Enzyme Rates and Bacterial Production	https://doi.org/10.1594/PANGAEA.926780	S16	Engel et al. (2021)
4.3.3 Microbial Oxygen Consumption, Nitrogen Transformation, and Primary Productivity Rates	https://doi.org/10.1594/PANGAEA.926781 https://doi.org/10.1594/PANGAEA.926785	S17 S18	Löscher and Mehrtens (2021a) Löscher and Mehrtens (2021b)
4.3.4 Marine Microbial Diversity and Function	https://www.ncbi.nlm.nih.gov	S19	
4.3.5 Zooplankton and Particle Distribution	https://doi.org/10.1594/PANGAEA.926794 https://doi.org/10.1594/PANGAEA.927040 https://doi.org/10.1594/PANGAEA.924375	S20 S21 S21	Hauss et al. (2021a) Kiko et al. (2021) Kiko et al.(2021)
4.3.6 Zooplankton Metabolic Rates	https://doi.org/10.1594/PANGAEA.927041	S22	Hauss et al. (2021b)
4.3.7 Nutrient amendment experiments	https://doi.org/10.1594/PANGAEA.927042	S23	Hauss et al. (2021c)
4.4 Paleoceanography	https://doi.org/10.1594/PANGAEA.927043 https://doi.org/10.1594/PANGAEA.927046 https://doi.org/10.1594/PANGAEA.927047 https://doi.org/10.1594/PANGAEA.927048 https://doi.org/10.1594/PANGAEA.927049	S24 S25 S26 S27 S28	Salvatteci and Mehrtens (2021a) Salvatteci and Mehrtens (2021b) Salvatteci and Mehrtens (2021c) Salvatteci and Mehrtens (2021d) Glock and Mehrtens (2021)

https://doi.org/10.5194/essd-2020-308
Preprint. Discussion started: 15 April 2021

4.5.1 In situ solute fluxes measured using the benthic flux lander BIGO	https://doi.org/10.1594/PANGAEA.928199	S29	M77/1-2	Sommer and Dale (2021a)
	https://doi.org/10.1594/PANGAEA.835700	S30	MSM17/4	Dale et al. (2014)
	https://doi.org/10.1594/PANGAEA.928204	S31	M92	Sommer and Dale (2021b)
	https://doi.org/10.1594/PANGAEA.928206	S32	M107	Sommer and Dale (2021c)
	https://doi.org/10.1594/PANGAEA.928280	S33	M136	Sommer and Dale (2021d)
	https://doi.org/10.1594/PANGAEA.928281	S34	M137	Sommer and Dale (2021e)
4.5.2 Near surface sediment coring	https://doi.org/10.1594/PANGAEA.928199	S29	M77/1-2	Sommer and Dale (2021a)
	https://doi.org/10.1594/PANGAEA.835700	S30	MSM17/4	Dale et al. (2014)
	https://doi.org/10.1594/PANGAEA.928204	S31	M92	Sommer and Dale (2021b)
	https://doi.org/10.1594/PANGAEA.928206	S32	M107	Sommer and Dale (2021c)
	https://doi.org/10.1594/PANGAEA.928280	S33	M136	Sommer and Dale (2021d)
	https://doi.org/10.1594/PANGAEA.928281	S34	M137	Sommer and Dale (2021e)
4.5.3 Metabolic rates of benthic microorganisms and their role in benthic N-cycling	https://doi.org/10.1594/PANGAEA.919751 https://doi.org/10.1594/PANGAEA.919839	S35		Glock (2020a) Glock (2020b)

4 Observational and experimental methods and data

During its 12-year existence, the SFB 754 used a large number of observational and experimental methods to assess the physical and biogeochemical state of the tropical oceans and the interactions between its components; these are briefly described here. Dataset collections have been created on PANGAEA for each of the following subsections (see Table 2). Each collection on PANGAEA also includes a pdf document with a summarizing table listing ancillary information and all relevant dataset DOIs. Table 1 lists the research cruises with their start and end dates together with the DOIs of the cruise reports where additional information about the data collected and methods used can be found.

https://doi.org/10.5194/essd-2020-308
Preprint. Discussion started: 15 April 2021

4.1 Physical Oceanography

Measurements of physical parameters in the surface layer and throughout the water column were a core element of the observational program of the SFB 754. They delivered information on the physical processes that determine the water masses and their properties in the regions of interest and at the same time set conditions for the various biogeochemical processes that determine the oxygen distribution.

4.1.1 Conductivity-Temperature-Depth-Oxygen (CTDO) measurements

CTDO measurements were acquired on 32 of the major research cruises performed as part of the SFB 754 or other projects (Krahmann and Mehrtens, 2021a; see Table 2 and supplementary Table S1). Seabird 911plus systems equipped with dual temperature-conductivity-oxygen sensors were employed. All systems had a 24-bottle water sampling rosette with 10 l Niskin bottles. On some cruises only 22 bottles were mounted to accommodate a lowered Acoustic Doppler Current Profiler for deep ocean current observations. Water sampling, processing, and calibration followed GO-SHIP recommendations (Swift, 2010; McTaggart et al., 2010; Uchida et al., 2010) and included the recommended steps *Data Conversion*, *Sensor Time-Alignment*, *Creation of Bottle Files*, *Outlier Removal*, *Pressure Sensor Filtering*, *Conductivity Cell Thermal Mass Correction*, *Ship Roll Correction and Deck Offset Correction by Loop Editing*, as well as *Derivation of Calculated Properties.* After these steps, conductivity and oxygen readings were calibrated against values determined with salinometry (see section 4.1.4) and Winkler titration (see section 4.2.1), respectively. Finally, the downcast data was averaged over 1 dbar wide intervals. An independent upcast calibration was used to obtain calibrated CTDO values coincident with the discrete water samples. These values entered the bottle file described in section 4.2.

In addition to the CTDO measurements, basically all CTDO casts included either a Dr. Haardt or a Wetlabs FLNTU fluorometer for CHL-a fluorescence. Several other sensors, such as a Wetlabs CDOM fluorometer and turbidity sensor, a Wetlabs C-Star transmissometer, a Photosynthetically Active Radiation (PAR) sensor manufactured by Biospherical Instruments, or a Seabird/Satlantic Submersible Ultraviolet Nitrate Analyzer (SUNA) have been attached to the CTDO system on some of the cruises or casts, depending on the availability of the sensors and their pressure ratings. SUNA data was processed

https://doi.org/10.5194/essd-2020-308
Preprint. Discussion started: 15 April 2021

following the procedures outlined in Sakamoto et al. (2009) and Sakamoto et al. (2017) and calibrated against Nitrate measurements from discrete bottle samples (see section 4.2.2). To CHL-a and CDOM fluorescence, turbidity, transmissometer beam attenuation, and PAR data only the manufacturer's calibration was applied in the published data sets. Details about the sensors used on each cruise can be found in the respective cruise reports (see Table 1).

4.1.2 Lowered Acoustic Doppler Current Profiler (LADCP) measurements

LADCP measurements were performed on all research cruises that concentrated on open ocean areas (Krahmann and Mehrtens, 2021b; see Table 2 and supplementary Table S2) while on cruises that worked mostly in shallow waters, ocean current measurements by the shipboard ADCP (see section 4.1.8) were deemed sufficient. GEOMAR used a two-instrument LADCP configuration with two Teledyne RDI 300 kHz workhorse ADCPs mounted in down- and up-looking positions. Data collection and processing was performed according to recommendations in the GO-SHIP manual (Thurnherr et al., 2010).

4.1.3 Moored instrument measurements

Almost all long-term moored observations of the SFB 754 were conducted in the tropical Atlantic between the equator and 18° N, except for one mooring that was deployed in the tropical South Pacific (Hahn et al., 2021; see Table 2 and supplementary Table S3). Moorings were typically equipped with instruments recording pressure, temperature, conductivity, dissolved oxygen, and current velocity. The moorings at 17.6° N, 24.2° W which have been deployed in the same location for several periods were additionally equipped with biogeochemical sensors recording variables such as partial pressure of CO_2 (pCO_2), fluorescence, and particle fluxes. Instruments with pressure, temperature, conductivity, and oxygen sensors were calibrated in situ immediately prior to and after a mooring deployment period by attaching them to the CTD frame during CTDO casts. Correction terms were then developed from the difference between the sensor readings and the calibrated CTDO data during several minute-long calibration stops. These correction terms were then applied to the full deployment periods. This ensured best data quality with recognition of potential sensor drifts and also allowed for the estimation of

https://doi.org/10.5194/essd-2020-308
Preprint. Discussion started: 15 April 2021

calibration and measurement errors (Hahn et al., 2014; Bittig et al., 2018; Berx et al., 2019). Moored Acoustic Doppler Current Profiler bin depths were corrected using the sound speed at instrument depth following the approach by Shcherbina et al. (2005). Velocities were not corrected, but respective measurement errors were assumed as described in Hahn et al. (2014). For all instruments within a mooring that did not record pressure, full deployment pressure time series were estimated by linearly interpolating between the instruments having a pressure sensor.

4.1.4 Salinometry

The conductivity sensors of the CTD were calibrated against IAPSO Standard SeaWater samples with known conductivities using Guildline Autosal B instruments. On all cruises two Autosals were available and used to measure between 100 and 1000 samples (typically 300–400 for a cruise or 4–5 per CTD cast). The procedures used for the calibration followed the recommendations in the GO-SHIP manual (Kawano, 2010). The results from the salinometer measurements are included in the source files for CTD data published on PANGAEA (Krahmann and Mehrtens, 2021a).

4.1.5 Autonomous Gliders

Autonomous gliders were deployed during several cruises but also as stand-alone missions independent from large research vessels (Krahmann and Mehrtens, 2021c; see Table 2 and supplementary Table S4). Two different generations of Teledyne Webb Research Slocum gliders were used, G1 and G2. All gliders were equipped with Seabird CTD systems, G1 gliders with an unpumped and G2 gliders with a pumped version, respectively. An Aanderaa optode was present on all gliders to observe dissolved oxygen concentrations. Optical fluorescence and backscatter sensors manufactured by Wetlabs were also present on all gliders albeit in different configurations. They allowed the determination of CHL-a (excitation and emission wavelengths of 470 and 695 nm, respectively) and CDOM (excitation and emission wavelengths of 370 and 460 nm, respectively) concentrations and the turbidity (scattering wavelength of 470 nm) of the waters. All glider data was processed using a GEOMAR-developed software (Thomsen et al., 2016) resulting in gridded fields for all observed variables. During a small number of glider deployments, a Seabird/Satlantic SUNA Nitrate sensor was attached to a glider.

https://doi.org/10.5194/essd-2020-308
Preprint. Discussion started: 15 April 2021

SUNA data was processed following the procedures outlined in Sakamoto et al. (2009) and Sakamoto et al. (2017) and calibrated against Nitrate measurements from nearby CTDO casts with discrete Nitrate measurements. Microstructure sensors were also attached to gliders on several deployments (see following section).

4.1.6 Ocean Turbulence Measurements

Ocean turbulence measurement programs were carried out during 22 cruises to quantify the dissipation rate of turbulent kinetic energy and infer rates of turbulent mixing (Dengler and Mehrtens, 2021; see Table 2 and supplementary Table S5). The shipboard microstructure profiling systems (MSS) were manufactured by Sea & Sun Technology and consisted of a profiler (MSS90-D, S/N 26, 32, and 73), a winch having 500–1000 m of cable and a data interface. All profilers were equipped with three microstructure shear sensors, a fast-response temperature sensor (PF07), an acceleration sensor, and two tilt sensors as well as conductivity (Sea & Sun Tech.), temperature (Sea & Sun Tech.), pressure (Keller), turbidity (Seapoint), and oxygen sensors sampling with a lower response time. The profilers were optimized to sink at a rate of 0.5–0.6 m s^{-1}. Standard processing procedures were used to determine the rate of kinetic energy dissipation of turbulence in the water column (see Schafstall et al., 2010).

Additionally, during several autonomous glider missions, a microstructure probe was mounted to the top of the gliders. These probes (MicroRider) were manufactured by Rockland Scientific and carried two microstructure shear and temperature sensors as well as pressure, accelerometer and tilt sensors. The data processing is detailed in Foltz et al. (2020).

4.1.7 Shipboard Acoustic Doppler Current Profiler (SADCP) measurements

SADCP data were acquired on 33 of the research cruises (Krahmann and Mehrtens, 2021d; see Table 2 and supplementary Table S6). On FS *Meteor*, FS *Maria S. Merian* and FS *Sonne II* two Teledyne RDI Ocean Surveyor systems with 38 and 75 kHz transmission frequency were used, while on NO *l'Atalante* a single 75 kHz system was used. All data was processed with a software package developed at GEOMAR following the GO-SHIP standards (Firing and Hummon, 2010). The data was subsequently

https://doi.org/10.5194/essd-2020-308
Preprint. Discussion started: 15 April 2021

averaged over one-minute intervals, converted to a NetCDF based format and published. For a small number of cruises, the signal strength information of the SADCP data has been used to estimate the backscatter in the ocean. These data sets were processed following Mullison (2017) and published separately from the regular SADCP data (Krahmann and Mehrtens, 2021d; see Table 2 and supplementary Table S6).

4.1.8 Underway Conductivity-Temperature-Depth (UCTD) and Rapidcast measurements

During the second funding phase (2012-2015) a new CTD system became available that could be deployed from a moving ship. First a Teledyne Oceanscience UCTD and later a Teledyne Oceanscience Rapidcast system were acquired and deployed successfully on several cruises (Krahmann and Mehrtens, 2021e; see Table 2 and supplementary Table S7). They allowed for the sampling of water masses at high horizontal resolution (ranging from less than 1 km for the Rapidcast system to 10 km for deep UCTD casts) with good accuracy of the pressure, temperature, and conductivity sensors. Processing of the data involved mostly the fall-rate dependent correction of the thermal lag of the conductivity sensor and followed the approach described by Ullman and Hebert (2014). Subsequently the corrected data was calibrated against the calibrated coincident Thermosalinograph (see subsequent section) and the calibrated nearby CTD data. The typical accuracies of the final pressure, temperature, and salinity data are 1 dbar, 0.01 °C, and 0.01 g/kg, respectively.

4.1.9 Thermosalinograph (TSG) measurements

For 32 SFB 754 cruises near-surface temperatures and salinities were collected using the ships' thermosalinograph systems. The four ships on which the major cruises were conducted were equipped with different systems with either one or two thermosalinographs in parallel or in alternating operating mode (Krahmann and Mehrtens, 2021f; see Table 2 and supplementary Table S8). All TSG data were cross-calibrated against the calibrated CTD data at the depth of the seawater intake for the TSG systems.

https://doi.org/10.5194/essd-2020-308
Preprint. Discussion started: 15 April 2021

4.1.10 Argo Floats

The SFB 754 also made a contribution to the global Argo float program (https://argo.ucsd.edu). In 2009, 2011, and 2014 several floats equipped with additional Aanderaa oxygen sensors were deployed off Peru to study the effects of mesoscale eddies on the flow field and the water masses (Czeschel et al., 2018; Krahmann and Mehrtens, 2021g; see Table 2 and supplementary Table S9). A number of floats was deployed in the tropical Atlantic to accompany a tracer release experiment (see section 4.2.3). Additionally several of the cruises were used to deploy regular Argo floats (without oxygen sensor) on behalf of the German Hydrographic Office.

4.2 Chemical Oceanography

The chemical oceanography program was comprehensive and included a range of different measurements whose scope was adapted to the different research questions of the cruises. While on all cruises measurements were performed on water samples from the CTD/rosette additional measurements were made on some cruises on water pumped continuously along the route of the ship. All cruises conducted oxygen measurements, almost all conducted nutrient measurements, while 9 conducted measurements of transient tracers and the deliberately released tracer CF_3SF_5. In addition, measurements of stable and radiogenic isotopes, the inorganic carbon system, nitrous oxide (N_2O), iodide, trace chemical species, and a range of other variables were conducted during the SFB 754. For a description of the not so frequently measured variables see the cruise reports (see Table 1).

4.2.1 Water sample oxygen measurements (Winkler titration)

A number of discrete samples were taken on most CTDO casts with the objective of calibrating the CTDO oxygen sensor (Tanhua and Mehrtens, 2021; see Table 2 and supplementary Table S10). Almost never were the full 24 (or 22 on cruises on which the LADCP was in use) Niskin bottles sampled, as an adequate calibration of the CTDO sensor could be achieved with fewer values. Samples were taken in 100 ml wide-necked WOCE glass bottles with well-defined volumes. Oxygen samples were taken immediately after the CTDO cast was finished and always directly after the sampling of transient tracers. The sample bottles were flushed with at least 3 times its volume and the samples were free of

https://doi.org/10.5194/essd-2020-308
Preprint. Discussion started: 15 April 2021

air-bubbles. Immediately after sampling, the seawater samples were spiked from the bottom with the fixation solution. A significant fraction of the discrete samples were taken as duplicates or triplicates in order to quantify sampling and titration uncertainties.

The oxygen concentration was determined by Winkler titration within a minimum of 40 minutes and a maximum of 16 hours after sampling following GO-SHIP best practices (Langdon, 2010). Details of oxygen measurements can be found in the cruise reports (Table 1) of the individual cruises. For all cruises, we followed the standard procedures for compensating for impurities in the reagents and oxygen in the fixation solution. For a few cruises with very low oxygen concentrations we compensated for the sampling blank, i.e. contamination from air during sampling and fixation, and outgassing from the PVC Niskin bottles.

4.2.2 Nutrient measurements

Nutrients were measured on-board for a sub-set of the cruises, and on another sub-set the samples were frozen for post-cruise processing in Kiel (Tanhua and Mehrtens, 2021; see Table 2 and supplementary Table S10). Nutrients measured on-board were performed with QuAAtro gas-segmented continuous flow analyzers (auto-analyzers) from SEAL Analytical. The exact methods used are listed in the cruise reports (see Table 1) and were normally: Nitrite and Nitrate – Q-068-05 Rev 11; Nitrite – Q-070-05 Rev 6; Phosphate – Q-064-05 Rev 8; Silicate – Q-066-05 Rev 5. The precision of the nutrient measurements was calculated as the average of the standard deviation from the replicate measurements of samples, and are recorded in the cruise reports. For the majority of the cruises where nutrients were measured on-board, reference Material for Nutrients in Seawater (RMNS) from the General Environmental Technos (KANSO) Co., Ltd., Osaka/Japan were used. Normally, reference material samples were measured as triplicates at least once in every sampling run. For nutrient analysis we followed the GO-SHIP best practices for nutrient measurements (Hydes et al., 2010).

4.2.3 Transient Tracer measurements

Three tracer release experiments were conducted during the SFB 754 using the artificial tracer CF_3SF_5; two in the tropical North Atlantic, and one in the tropical South Pacific (Tanhua and Mehrtens, 2021;

https://doi.org/10.5194/essd-2020-308
Preprint. Discussion started: 15 April 2021

see Table 2 and supplementary Table S10). The analytical technique for measuring this tracer is similar to that of the transient tracers CFC-12 and SF_6. Both transient (i.e. CFC-12 and SF_6) and released (CF_3SF_5) tracers were measured on 9 of the SFB 754 cruises. The tracers were measured using gas chromatograph / purge-and-trap techniques modified from Bullister and Weiss (1988). The sampling for CF_3SF_5 was focused around the density where the tracer was released, whereas the transient tracers sampling covered the whole depth of the CTDO profiles. The sampling volume for transient tracers was around 200 ml, whereas the sampling volume for CF_3SF_5 varied with time after injections (i.e. based on the expected concentration range) from 20 to 1000 ml.

4.2.4 Water column measurements of N_2O

Extensive discrete sampling for measurements of N_2O was carried out on seven cruises during the time span of the SFB 754 (Tanhua and Mehrtens, 2021; see Table 2 and supplementary Table S10). Samples were collected with either the CTD/Rosette or a pump-CTD system (see Löscher et al., 2012; Kock et al., 2016) and measured directly on board or at the Chemical Oceanography department of GEOMAR. Samples were analysed by means of a headspace equilibration method coupled to gas chromatography with electron capture detection (for details, see Kock et al., 2016 and references therein).

4.2.5 Dissolved Silicate, Nitrate, and Nitrite Isotopes

Seawater samples for stable isotopes measurements of dissolved silicate ($\delta^{30}Si$), nitrate ($\delta^{15}NO_3^-$) and nitrite ($\delta^{15}NO_2^-$) were taken from the CTD/rosette on a number of SFB 754 cruises (Grasse et al., 2021; see Table 2 and supplementary Table S11). Samples for $\delta^{30}Si$ were taken during M77/3, M77/4, M90, and M93 and immediately acidified to pH 2 after filtration (Ehlert et al., 2012; Grasse et al., 2013; Grasse et al., 2016). Sample preparation was according to the GEOTRACES (https://www.geotraces.org) protocol and samples for $\delta^{30}Si$ were measured at GEOMAR on a Nu Plasma MC-ICP-MS (Nu Instruments™, Wrexham, UK). $\delta^{15}NO_3^-$ and $\delta^{15}NO_2^-$ samples were taken during M77/3, M77/4, M90, M92 and M93. The samples were either preserved frozen or an azide treatment was applied depending on the nitrite concentration (Altabet et al., 2012; Bourbonnais et al.,

https://doi.org/10.5194/essd-2020-308
Preprint. Discussion started: 15 April 2021

2015; Hu et al., 2016; Ryabenko et al., 2012). The isotopic composition of both N-species was measured using the Cd reduction/azide method (McIlvin and Altabet, 2005).

4.2.6 Radiogenic Isotopes

Seawater samples for Rare Earth Element (REE) concentrations and neodymium (Nd) isotopes were taken during M77/3 and M77/4 off Peru (Grasse et al., 2012) and during M90 in the Panama Basin (Grasse et al., 2017; Grasse et al., 2021; see Table 2 and supplementary Table S12). Samples were taken with the CTD rosette and filtered through 0.45 µm nitrocellulose acetate filters (Millipores) shortly after sampling. For analysis of Nd isotopes 20 l of seawater were collected for each sample and treated following GEOTRACES protocol (van de Flierdt et al., 2012). Nd isotope measurements were carried out on a Nu plasma MC-ICPMS as well as on a Thermo Scientific TIMS TRITON. The concentrations of dissolved REEs in seawater were measured with a SeaFAST online preconcentration system (Elemental Scientific Inc.) connected to an Agilent 7500ce quadrupole ICP-MS at GEOMAR (Hathorne et al., 2012).

4.2.7 Underway trace gas measurements

Continuous measurements of the climate-relevant trace gases carbon dioxide (CO_2), nitrous oxide (N_2O), and carbon monoxide (CO) in the surface ocean and overlying atmosphere were conducted during 9 SFB 754 cruises (Arévalo-Martínez and Mehrtens, 2021; see Table 2 and supplementary Table S13) spanning the North, South and equatorial Atlantic, as well as the South and equatorial Pacific. To this end, laser spectroscopy-based gas analysers coupled to air-water equilibration chambers were used. For details of the analytical systems the reader is referred to the descriptions provided by Arévalo-Martínez et al. (2013) and Arévalo-Martínez et al. (2019). All trace gas measurements were quality-controlled to achieve the international standards for marine CO_2 (Bender et al., 2002), N_2O (Bange et al., 2019), and atmospheric CO (Zellweger et al., 2019; to date there is no accepted standard for seawater measurements). The final quality-controlled data is available through the Surface Ocean CO_2 Atlas (SOCAT, https://www.socat.info/) and the Marine CH_4-N_2O database (MEMENTO,

https://doi.org/10.5194/essd-2020-308
Preprint. Discussion started: 15 April 2021

https://memento.geomar.de/) as well as on PANGAEA (Arévalo-Martínez and Mehrtens, 2021; see Table 2 and supplementary Table S13).

4.2.8 Trace chemical species

Trace metal clean sampling equipment was deployed on a sub-set of cruises (see Croot et al., 2021; see Table 2 and supplementary Table S14) to facilitate the observation of contamination prone chemical parameters. All trace metal sample collection, handling, and analysis was conducted in accordance with GEOTRACES protocols which have been updated through the SFB754 program (Cutter et al., 2014). For cruises with extensive trace metal work, the deployment of an over-pressured clean container on deck facilitated sampling and collection of trace metal and other contamination-prone samples at sea. For cruises from 2008 to 2013, PTFE-coated 8 l GO-FLO bottles (General Oceanics) were mounted on a Kevlar wire with sample handling and preservation as per Chever et al. (2015). From 2014 onwards, 24 Ocean Test Equipment (OTE) samplers were deployed mounted on a powder coated sampling CTD (Sea-Bird SBE25) rosette using a Kevlar conducting cable with sample handling and preservation as per Rapp et al. (2019).

Prior to 2014, dissolved trace metal concentrations were largely determined by graphite furnace atomic absorption spectroscopy after offline pre-concentration as per Schlosser et al. (2018) with calibration of all elements via standard addition. Post 2014, dissolved trace metal samples were analysed via Inductively Coupled Plasma Mass Spectrometry after offline pre-concentration using a SEAFAST system exactly as per Rapp et al. (2017). A number of trace metal isotopes were also analysed with forthcoming datasets expected to expand the limited available isotopic data for the Peruvian OMZ with analysis as per Chever et al. (2015) for Fe and Xie et al. (2019) for Cd.

In addition to dissolved trace metal concentrations, a number of redox sensitive trace species were quantified. These included Fe(II) and H_2O_2concentrations determined using flow injection analysis (Croot et al., 2019; Schlosser et al., 2018), and other Reactive Oxygen Species as per Wuttig et al. (2013). Metal-speciation was also explored through titrations to characterize metal-ligand interactions with analytical methods as per Baars and Croot (2015) for Co species, and Gledhill and Van Den Berg (1994) for Fe(III) species.

https://doi.org/10.5194/essd-2020-308
Preprint. Discussion started: 15 April 2021

4.3 Biological Oceanography

Pelagic biological field work of varying extent was carried out during most cruises. Topics spanned from marine biogeochemistry and microbiology to zooplankton and nekton ecology, and methods included field observations as well as on-board incubations for microbial as well as metazoan metabolic rate determination and large-scale experimental set-ups with various treatments such as bioassays, shipboard mesocosms and a mesocosm experiment off Callao using the KOSMOS system.

4.3.1 Particulate Organic Matter and Pigment Analysis

Particulate organic matter (POM) distribution in the water column was on several cruises (Engel and Mehrtens, 2021; see Table 2 and supplementary Table S15) determined after filtration onto pre-combusted, acid-washed GF/F filters (Franz et al., 2012a). For particulate organic carbon (POC) and particulate nitrogen (PN), filters were exposed to fuming hydrochloric acid for 12 h to remove carbonate and subsequently dried (60 °C, 12 h). Analyses were carried out with a Euro EA elemental analyzer calibrated with an acetanilide standard. Particulate organic phosphorus (POP) collected on GF/F filters was determined colorimetrically as ortho-phosphate after potassium peroxydisulphate digestion following the method of Hansen and Koroleff (1999). Biogenic silica (BSi) was determined from material filtered onto cellulose acetate filters (0.8 µm), dissolved with 25 ml NaOH (0.1 M) at 85 °C for 2h 15 min in a shaking water bath and analysed after cooling as $Si(OH)_4$ according to the method by Hansen and Koroleff (1999). Biogenic opal was calculated assuming a watercontent of ~10% (Mortlock and Fröhlich, 1989).

Samples for phytoplankton pigment concentrations were collected by filtration of seawater from the CTD/rosette through GF/F filters, and stored at -80 °C immediately after filtration. Pigments were extracted and analysed by High Performance Liquid Chromatography (HPLC) (Franz et al., 2012a). Seawater samples (4 ml) were collected for analyses of the phytoplankton community composition by flow cytometry to complement phytoplankton pigment data, fixed with hexamine/formalin solution and stored at -80 °C.

Transparent exopolymer particles (TEP) and Coomassie stainable particles were filtered under low pressure (< 150 mbar) onto 25 mm Nuclepore membrane filters (0.4 µm pore size, Whatman Ltd.) and

https://doi.org/10.5194/essd-2020-308
Preprint. Discussion started: 15 April 2021

stained with Alcian Blue and Coomassie Brilliant Blue, respectively. Each filter was placed on the white side of a semi-transparent glass slide (Cytoclear©) and stored frozen at -20 °C until analysis. TEP and CSP were determined by microscopy and subsequent image analysis (Engel, 2009).

Export flux of was characterized using surface-tethered sediment traps (Engel et al., 2017), with Particle Interceptor-Traps (PIT) following Knauer et al. (1979). Each PIT had an inside diameter of 7 cm, an outside diameter of 7.6 cm and a height of 53 cm, leading to an aspect ratio of 7.5. PITs were covered with a baffle system consisting of smaller acrylic tubes attached to the top end and filled with a 0.2 µm filtered brine solution containing 50 g l^{-1} sodium chloride to reduce drag-induced movement within the trap. For preservation, formalin (2% final concentration) was added to the brine solution.

4.3.2 Dissolved Organic Matter, Cell Abundance, Extracellular Enzyme Rates, and Bacterial Production

For dissolved organic carbon (DOC) and total dissolved nitrogen (TDN), samples (20 ml) were collected in duplicate on a number of cruises (Engel et al., 2021; see Table 2 and supplementary Table S16), filtered through combusted (8 h, 500 °C) GF/F filters or through syringe filters (0.45 µm glass microfiber GD/X membrane, Whatman™) that were rinsed with 50 ml sample and filled into combusted (8 h, 500 °C) glass ampoules. Samples were acidified with 80 µl of 85 % phosphoric acid or 20 µl of 30 % ultrapure hydrochloric acid, heat-sealed immediately and stored at 4 °C in the dark until analysis. DOC samples were analyzed by high-temperature catalytic oxidation (TOC-VCSH, Shimadzu), as described in more detail in Engel and Galgani (2016).

Samples for the analysis of dissolved amino acids (DAA, ~4 ml) and dissolved combined carbohydrates (DCHO, ~16 ml) were filtered through rinsed Acrodisc® 0.45 µm GHP membrane (Pall) in combusted vials (8 h, 500 °C) and stored at -20 °C, respectively. Prior to analysis DAA were hydrolysed using 6 N HCl at 100 °C for 20 h. Determination of DAA was carried on a 1260 HPLC system (Agilent), following the methods described by Lindroth and Mopper (1979) and Dittmar et al. (2009), with modifications as described in Engel and Galgani (2016). DCHO samples were desalted by membrane dialysis (1 kDa, Spectra Por) and hydrolysed using 1 M HCl for 20 h at 100 °C prior to analyses. Samples were analysed after Engel and Händel (2011) with a high-performance anion exchange

https://doi.org/10.5194/essd-2020-308
Preprint. Discussion started: 15 April 2021

chromatography (HPAEC) (DIONEX ICS3000DC). More detail on molecular DOM composition may be found in Loginova et al. (2019) and Maßmig et al. (2020).

Bacterial abundance was determined by flow cytometry on a FACS Calibur (Becton Dickinson) after Gasol and Del Giorgio (2000) from 1.6 ml sample, fixed with 0.75 µl 25 % glutaraldehyde on board and stored at -80 °C until analyses. To 400 µl sample 10 µl Flouresbrite® fluorescent beads (Polyscience, Inc.) and 10 µl Sybr Green (Invitrogen) were added.

For the extracellular enzymes leucine aminopeptidase and *ß*-glucosidase, potential hydrolytic rates were determined after Hoppe (1983). L-leucine-7-amido-4-methylcoumarin (Sigma Aldrich) and 4-methylumbelliferyl-ß-D-glucopyranoside (Acros Organics) were used as fluorescent substrate analogs and added in final concentrations of 1, 5, 10, 20, 50, 80, 100, and 200 µmol l^{-1} in 69 well plates (Costar). Afterwards 200 µl sample were added and fluorescence was measured with a plate reader fluorometer (FLUOstar Optima, BMG labtech) (excitation: 355 nm; emission: 460 nm) after 0 and 12 h of incubation. For details about incubation conditions and subsequent calculations see Maßmig et al. (2020).

Bacterial production was determined by measuring the incorporation of labeled leucine (3H) that was added at a saturating final concentration of 20 nmol (specific activity 100 Ci $mmol^{-1}$, Biotrend) in 1.5 ml of sample (Kirchman et al., 1985; Smith and Azam, 1992). After 3 hours of incubation, samples were measured with a liquid scintillation counter (Hidex 300 SL, TriathalerTM,FCI). For the estimation of incorporated carbon, a conversion factor of 1.5 kg C mol^{-1} leucine was used (Simon and Azam, 1989). For further details about incubation conditions, sample treatment and subsequent calculations see Maßmig et al. (2020).

FDOM samples were filtered through 0.2 µm polyethersulfone syringe filters (CHROMAPHIL® Xtra PES-45/25) and stored into 15 ml combusted (450 °C, 8 h) amber-glass vials and at -20 °C.

FDOM was determined using 3D-Excitation-Emission-Matrix (EEM) fluorescence spectroscopy followed by parallel factor analysis (PARAFAC). EEM spectra were obtained using a Cary Eclipse Fluorescence Spectrophotometer (Agilent Technologies) within 230–455 nm excitation wavelength range in 5 nm intervals and within 290–700 nm emission wavelength range in 2 nm intervals. All FDOM samples were brought to the room temperature before analyses, the measurements were

https://doi.org/10.5194/essd-2020-308
Preprint. Discussion started: 15 April 2021

performed under temperature-controlled conditions at 19 °C using Cary Single Cell Peltier Accessory (VARIAN). All the fluorescence measurements were performed at 0.2 s integration times and 5 nm slit width on both monochromators.

The 3D fluorescence spectra were corrected and analysed by PARAFAC (Stedmon and Bro, 2008), using "drEEM toolbox for MATLAB" after Murphy et al. (2013). The humification and biological indexes were calculated after (Zsolnay et al., 1999). CDOM samples were collected into combusted (450 °C, 8 h) 40 ml amber-glass vials. All samples were passed through 0.2 µm polyethersulfone syringe filters (CHROMAPHIL® Xtra PES-45/25, MACHEREY-NAGEL GmbH & Co.KG) before storage at 4 °C. Samples were processed within 1–90 days. The measurements were performed at room temperature (~19 °C) using Shimadzu® 1800 UV-VIS double-beam spectrophotometer within 230–750 nm wavelength range against MilliQ water at 1 nm intervals. More details on the spectroscopic analyses may be found in Loginova et al. (2015, 2016, 2020).

4.3.3 Microbial Oxygen Consumption, Nitrogen Transformation and Primary Productivity Rates

Dinitrogen (N_2) and carbon (C) fixation rates were measured on 9 cruises (Löscher and Mehrtens, 2021a; see Table 2 and supplementary Table S17) using shipboard incubation experiments, complemented with nutrient and oxygen manipulations. During cruises M77/3, M77/4, and M80/2, N_2 fixation was measured using the bubble addition method following Montoya et al. (1996). During M80/2 a novel method based on $^{15}N_2$ gas pre-dissolution, which was developed by Mohr et al. (2010), was tested in parallel to the classic method. An underestimation of N_2 fixation rates by the classic method has been observed (Großkopf et al., 2012) and therefore the novel 'pre-dissolution method' was applied during the following cruises (M83/1, M90, M91, M93, M97, M104, M107). Single cell N_2 fixation rates to differentiate the contribution of different clades of N_2 fixers were measured using a NanoSIMS (Martinez-Perez et al., 2016). C fixation was determined using ^{13}C- bicarbonate additions (e.g. Grosskopf et al., 2012; Löscher et al., 2014) and heterotrophic C turnover was determined using ^{13}C- glucose additions (Löscher et al., 2014, 2016).

https://doi.org/10.5194/essd-2020-308
Preprint. Discussion started: 15 April 2021

Potential rates for microaerobic respiration and aerobic organic matter degradation as a source of ammonia (NH_4^+) in the Peruvian OMZ was assessed using an $^{18}O_2$ labelling approach suitable for microaerobic respiration (Holtappels et al., 2014). Further, the effects of O_2 depletion associated with marine snow particles on microbial respiration was explored by combining $^{18}O_2$ labelling experiments with in-situ particle size analysis and modelling of aggregate-size dependent respiration (Kalvelage et al., 2015). Anammox, denitrification, and nitrification, as well as N_2O production rates were measured on several cruises (Kalvelage et al., 2011; Löscher et al., 2012; Callbeck et al., 2017; Bourbonnais et al., 2017; Frey et al., 2020; Löscher and Mehrtens, 2021b; see Table 2 and supplementary Table S18) using isotope fractionation studies, ^{15}N tracer additions, and inhibitor studies.

4.3.4 Marine Microbial Diversity and Function

In order to identify key groups of microbes for C, N, and O_2 turnover, microbial metabolic rate measurements were complemented with analyses of metagenomes and metatranscriptomes from the Eastern Tropical South Pacific (ETSP) and Eastern Tropical North Atlantic (ETNA). In addition, key gene and transcript characterization and quantification for aerobic respiration (Kalvelage et al., 2015), N_2 fixation (Großkopf et al., 2012; Löscher et al., 2014, 2015, 2016, 2020), anammox, denitrification and nitrification (Kalvelage et al., 2013, Löscher et al., 2012, 2015, 2016) were carried out using Sanger sequencing and quantitative real time polymerase chain reactions (PCRs) as described in Löscher et al., (2012, 2014). To assure high quality sampling of nucleic acids, sample filtration times did not exceed 20 min and samples were shock-frozen in liquid N_2 and stored at -80 °C (e.g., Löscher et al., 2014). Early metagenomic and -transcriptomic analyses targeted an understanding of microbial communities in the surface waters above the OMZ, the oxyclines, OMZ core waters, and sulfidic anoxic waters, as summarized in Löscher et al. (2016) and were based on Pyrosequencing technology (e.g., Schunck et al., 2013; Desai et al., 2013). Due to the rapid advance in sequencing technologies, it was possible to generate more conclusive metagenomes for targeted studies on sulphur, N, and O_2 cycling during M90–M93. Nine metagenomes were sequenced using Illumina HiSeq technology (Callbeck et al., 2018) from those cruises. On those datasets, genome assemblies and phylogenetic classifications were carried out to explore the role of a key microbial cluster, SUP05, and its role in OMZ sulphur and nitrogen

https://doi.org/10.5194/essd-2020-308
Preprint. Discussion started: 15 April 2021

turnover. Metagenomes from the ETNA cruise M107 were sequenced in the context of the development of anoxic water masses in collaboration with the DFG-funded Cluster of Excellence 'The Future Ocean' (Löscher et al., 2015). In addition to full metagenomes, targeted community studies were carried out using 16S rDNA amplicon sequencing sequenced on Illumina MiSeq sequencers from the same anoxic eddy in the ETNA and from the Peruvian OMZ (Löscher et al., 2015; Scholz et al., 2016). All published sequences were submitted to the National Center for Biotechnology Information's archives (NCBI; https://www.ncbi.nlm.nih.gov/; see Table 2 and supplementary Table S19). Physical DNA libraries were generated, and subsamples are available on request from C. Löscher.

In addition to this mainly pelagic work, transcriptomes, and genomes of the denitrifying benthic foraminifera *Globobulimina turgida* and *G. auriculata* from the seasonally hypoxic Swedish Gullmar Fjord were analysed (Woehle and Roy et al., 2018). The obtained information was used to describe the foraminifera unique eukaryotic ability to denitrify and colonize low-oxygen environments. Sequences were submitted to the NCBI's Sequence Read Archive (accession numbers SRR6202052 - SRR6202078) and to the transcriptome sequencing archive (accession numbers GGCE00000000 and GGCD00000000). The genome assembly was submitted to NCBI (draft genomes PIVH00000000-PIWH00000000; unassigned contigs: PJEL00000000). Furthermore, individually amplified 18S rRNA gene sequences of the two analysed foraminiferal species were submitted to GenBank (MG800664 to MG800667).

4.3.5 Zooplankton and Particle Distribution

A Hydrobios Multinet Midi with an aperture of 0.25 m^2 and 5 nets (mesh size 200 µm) was deployed for vertically stratified hauls on several cruises (Hauss et al., 2021a; see Table 2 and supplementary Table S20), mostly in paired day-night hauls to quantify diel vertical migration. Standard depths used for these deployments were 1000-600-300-200-100-0 m. On cruise M93, a Multinet Maxi (9 nets, 333 µm mesh) was used instead. Samples were fixated in 4% formaldehyde in seawater solution, scanned at GEOMAR or at the Ocean Science Center Mindelo, Mindelo/Cape Verde, and analyzed using automated imaging software (Gorsky et al., 2010) allowing taxonomical classification as well as the estimation of taxon-specific biomass (Lehette and Hernández-León, 2006) and metabolic rates. Scanned

https://doi.org/10.5194/essd-2020-308
Preprint. Discussion started: 15 April 2021

image data are available on EcoTaxa (https://ecotaxa.obs-vlfr.fr/; Picheral et al., 2017) upon request from R. Kiko and H. Hauss. Taxon-specific biomass and metabolic rate estimates are publicly available on PANGAEA (Kiko and Hauss, 2019; Kiko et al., 2020).

To expand the ecological knowledge on fragile organisms (such as giant rhizaria, medusae, ctenophores, and siphonophores) in situ imaging techniques were employed in addition to net sampling. An Underwater Vision Profiler 5 (UVP5; Picheral et al., 2010) was routinely mounted on the CTD/rosette during most SFB 754 cruises since 2012 (Kiko et al., 2021a; see Table 2 and supplementary Table S21). During the cruises in 2012 and 2013 a UVP5 was used that was kindly provided by the Laboratoire d'Océangraphie de Villefranche-sur-Mer (France). The instrument consists of one down facing HD camera in a steel pressure case and two red LED lights which illuminate a 0.88 to 0.93 l volume (depending on the actual set-up). During the downcast, the UVP5 takes 3–20 pictures of the illuminated field per second. For each picture, the particles are counted and sized immediately and the data is stored in the instrument for later analysis. Furthermore, images of particles with a size >500 µm are saved as separate "vignettes" - small cut-outs of the original picture - which allow for later, computer assisted, identification of these particles and their assignment into different particle, phyto-, and zooplankton groups. Since the UVP5 was integrated in the CTD and has its own pressure sensor, fine-scale vertical distribution of particles and major planktonic groups can be related to environmental data. UVP5 particle and zooplankton data from all cruises can be accessed on EcoTaxa (https://ecotaxa.obs-vlfr.fr/; Picheral et al., 2017). UVP5 particle data has undergone further quality controls since their first publication and were merged with data from other international collaborators to yield a global dataset. This dataset, to be found at https://doi.org/10.1594/PANGAEA.924375 supersedes the previous UVP5 particle datasets and should be used for further research, whereas the original datasets are still available for reference.

4.3.6 Zooplankton Metabolic Rates

Zooplankton metabolic rates (oxygen respiration and ammonium excretion) at different temperatures, oxygen, and carbon dioxide partial pressures (Kiko et al., 2015; 2016) were measured during three cruises (Kiko et al., 2021b; see Table 2 and supplementary Table S22). Zooplankton was collected by

https://doi.org/10.5194/essd-2020-308
Preprint. Discussion started: 15 April 2021

different nets and the entire catch immediately transferred to 10 l beakers containing pre-cooled seawater. Diel vertical migrators were sampled at the surface at night. Individuals for respiration rate measurements were isolated immediately and maintained in filtered seawater for 1 to 13 hours at the chosen experimental temperature (13, 18, or 23 °C). Only animals appearing unharmed and fit were used for experiments. Water for the respiration and excretion rate trials was UV-treated, filtered over a 0.2 µm sterile filter, and supplemented with antibiotics (25 mg l^{-1} ampicillin and 25 mg l^{-1} streptomycin). Subsequently, the water was bubbled with different Gas mixtures (N_2, O_2, CO_2; see Kiko et al., 2016 for details) adjusted to represent different environmental pO_2 and pCO_2 levels. Incubation bottles (12 to 280 ml) were pre-filled with the respective incubation water and the animals quickly added, transferring as little water as possible. The incubation bottles were equipped with a PreSense oxygen microsensor spot and readout was conducted from the outside, using a fibre optic cable and a 4- or 10-channel Oxy-Mini (PreSens Precision Sensing GmbH, Regensburg, Germany). Incubations were conducted in the dark in 10 l water baths located inside temperature-controlled incubators. Experiments were generally conducted for a maximum of 16 hours to avoid microbial growth, which would have affected the ammonium measurements. Generally, three incubations were combined with one animal free control incubation, which served to estimate microbial background respiration and ammonium concentrations in these controls. As oxygen levels within the bottles declined, respiration rates could also be estimated at other than the pre-set conditions. After an acclimation phase of 1 hour, respiration rates were calculated for 1-hour intervals using a linear regression. The microbial background respiration rate was subtracted from the experimental incubation respiration rate to yield the animal's respiration rate. Generally, 1 or 15 ml water samples were taken at the end of the incubation to determine ammonium concentrations fluorometrically according to Holmes et al. (1999). Ammonium excretion rates were calculated as the difference between the incubation and animal-free controls. Animals used in the experiments were afterwards recovered, frozen at -80 °C and transported to the home laboratory, where their dry-weight was determined. The rates presented should be considered routine metabolic rates, as activity was not monitored continuously (Prosser, 1961). Please refer to Kiko et al. (2015, 2016) for further experimental details.

https://doi.org/10.5194/essd-2020-308
Preprint. Discussion started: 15 April 2021

4.3.7 Nutrient amendment experiments

Bioassays with amendment of DIN, DIP, and various trace elements were conducted in short-term replicated bottle incubations to determine limiting elements for phytoplankton growth (Browning et al., 2017; Hauss et al., 2021b; see Table 2 and supplementary Table S23). Shipboard mesocosm experiments with a duration from 7 to 11 days were conducted on several cruises in the ETNA and ETSP and land-based on Cape Verde to determine the impact of N:P stoichiometry on the pelagic community (Franz et al., 2012b; Hauss et al., 2012; Czerny et al. 2016; Meyer et al., 2016) and dissolved organic compounds (Loginova et al., 2015; Engel et al., 2015). In austral summer 2017, a large-scale in situ mesocosm experiment was conducted off Callao (Peru) using the KOSMOS facilities. Deep water was injected into the mesocosms to simulate an upwelling event and the response of the planktonic ecosystem was monitored for 50 days (Bach et al., 2020).

4.4 Paleoceanography

One of the objectives of the SFB 754 was the reconstruction of the factors controlling the intensity and the spatial extent of the OMZ in the Eastern Tropical Pacific, specifically off Peru, since the Last Glacial Maximum (21000 years ago). For the purpose of these paleoceanographic studies, long gravity cores were recovered during four scientific expeditions (M77/1, M77/2, M92, and M135; see Figure 4). During the cruises M77/1 and M77/2 in 2008, 51 sediment cores were retrieved below and in the centre of the OMZ, from ~17° S to the equator (Pfannkuche et al., 2011; see Figure 4). Most of the records collected in the core of the OMZ (i.e. ~200 to ~500 m depth), from ~8 to 15° S, show sedimentary discontinuities during the Holocene (last 11700 years), which preclude high resolution paleoceanographic reconstructions in this area (Erdem et al., 2016; Salvatteci et al., 2014, 2016). Based on the information collected during M77/1 and M77/2 and also on the scientific literature, cruise M135 aimed specifically at finding the most complete Holocene sequence in the Eastern Tropical South Pacific. For this purpose, a detailed paleoceanographic survey took place at ~17° S, an area that is less affected by processes that can produce sediment discontinuities. Six sediment cores were retrieved, two

https://doi.org/10.5194/essd-2020-308
Preprint. Discussion started: 15 April 2021

of which contained the most complete sediment sequences for the last 10000 years (Salvatteci et al., 2019).

Data from the gravity and piston cores taken during cruises M77/1, M77/2, M92, and M135 has been assembled by Salvatteci and Mehrtens (2021a; see Table 2 and supplementary Table S24). A piston corer was used on cruise M77/2 while on M77/1, M92, and M135 a long gravity corer was employed. In total 57 sediment cores were taken on the three cruises. The water depths of the sampling sites ranged from 144 to 2591 m; however, most of the cores were retrieved in the core of the OMZ, i.e. between ~200 and ~700 m depth. The average sediment recovery of the piston cores was 1168 cm. For the gravity cores, the average sediment recovery was 318 cm for M77/1 and 609 cm for M135. Up to date, these sediment cores have been used in 17 scientific publications that aim to understand climate and ocean variability and its effect on the OMZ at multiple timescales (Salvatteci and Mehrtens, 2021a; see Table 2 and supplementary Table S24). Age models (Salvatteci and Mehrtens, 2021b; see Table 2 and supplementary Table S25), X-Ray Fluorescence (XRF) measurements (Salvatteci and Mehrtens, 2021c; see Table 2 and supplementary Table S26), and other geochemical records (Salvatteci and Mehrtens, 2021d; see Table 2 and supplementary Table S27) have been assembled and published. In addition, core tops of near sediment surface cores from multiple-corers (MUCs) have been used to establish local calibrations for several paleoproxies, such as redox-sensitive elements in foraminifera (i.e. Mn/Ca, I/Ca and Fe/Ca), foraminiferal assemblages, and stable Mo and N isotopes (Glock and Mehrtens, 2021; see Table 2 and supplementary Table S28).

https://doi.org/10.5194/essd-2020-308
Preprint. Discussion started: 15 April 2021

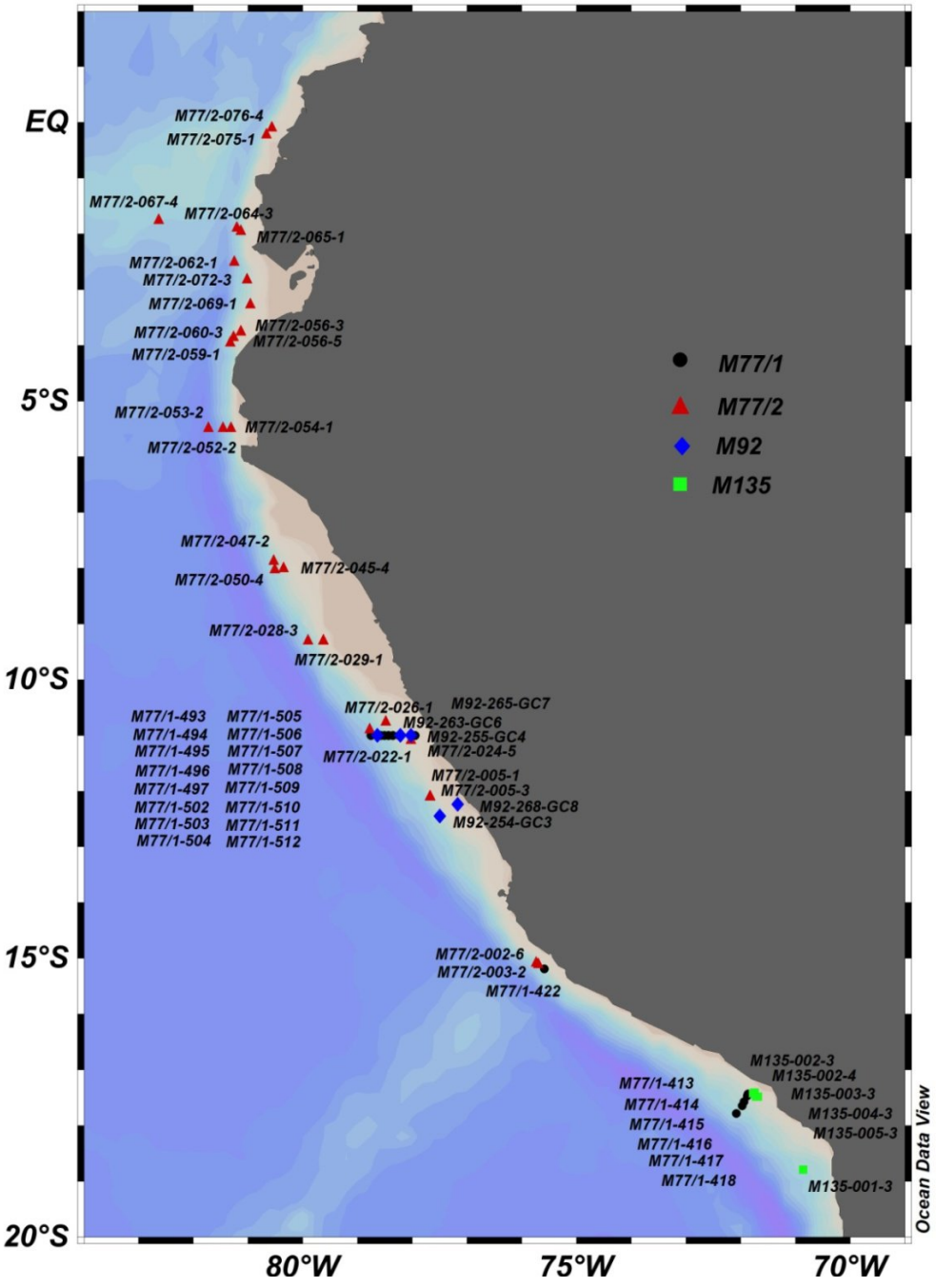

Figure 4. Map of the Eastern Tropical South Pacific showing the location of the gravity cores and piston cores taken during cruises M77/1 (black circles), M77/2 (red triangles), M92 (blue diamonds)and M135 (green squares).

https://doi.org/10.5194/essd-2020-308
Preprint. Discussion started: 15 April 2021

4.5 Benthic fluxes and surface sediment sampling

In the Peruvian upwelling area, benthic biogeochemical fieldwork focused on the FS *Meteor* cruises M77/1, M77/2, M92, M136, and M137. Off Mauritania, benthic investigations were mainly conducted on FS *Maria S. Merian* cruise MSM17/4 and FS *Meteor* cruise M107 (Sommer et al., 2021; see Table 2 and supplementary Tables S29 to S35). Research questions addressed organic carbon degradation, associated element cycling, and solute fluxes in the benthic boundary layer in response to variable bottom water redox conditions and hydrodynamic forcing (e.g. Bohlen et al., 2011; Dale et al., 2014; Dale et al., 2016; Dale et al., 2019; Dale et al., 2021; Loginova et al., 2020; Lomnitz et al., 2016; Noffke et al., 2012; Plass et al., 2020; Schroller-Lomnitz et al., 2019; Sommer et al., 2016). Effects of variable bottom water conditions on seabed nutrient and trace metal release were studied during in situ and ex situ on-board sediment incubations and the analysis of pore water geochemistry. Further emphasis was placed on resolving the imprint of specific microbial processes and foraminiferal metabolic activity on element turnover and exchange across the sediment water interface (e.g. Glock et al., 2013, 2019, 2020; Gier et al., 2016, 2017; Scholz et al., 2016; 2017). The results were further interpreted using benthic numerical models (e.g. Bohlen et al., 2011; Dale et al., 2014, 2015, 2016, 2017, 2019). The corresponding DOIs are listed in the supplementary Tables S29 to S35.

4.5.1 In situ solute fluxes measured using the benthic flux lander BIGO

Benthic solute fluxes of major elements traversing the Peruvian OMZ at 11° S and 12° S were determined based on data measured in situ using the two Biogeochemical Observatories BIGO I and BIGO II during FS *Meteor* cruises M77/1-2 (2008, 11° S; Pfannkuche et al., 2011; see also supplementary Table S29), M92 (2013, 12° S; Sommer et al., 2014; see also supplementary Table S31), M136 (2017, 12° S; Dengler and Sommer, 2017; see also supplementary Table S34) and M137 (2017, 12° S; Sommer et al., 2019; see also supplementary Table S35). Solutes fluxes along a zonal transect at 18° N off Mauritania were determined during the FS *Maria S. Merian* cruise MSM17/4 in 2011 (Pfannkuche, 2014; see also supplementary Table 30) and FS *Meteor* cruise M107 in 2014 (Sommer et al., 2015; see also supplementary Table S32). The landers are described in detail by Pfannkuche and

https://doi.org/10.5194/essd-2020-308
Preprint. Discussion started: 15 April 2021

Linke (2003) and Sommer et al. (2008, 2009, 2016). Note that during the cruises M77/1-2 the landers were named BIGO and BIGO T instead of the usual terminology of BIGO I and BIGO II .

During all cruises the basic functioning principle of the BIGO type lander was the same. However, for some measurements and experiments the lander set-up was modified slightly. Details of the modifications are provided in cruise reports and specific publications. In brief, the BIGO lander contained two circular flux chambers (internal diameter 28.8 cm, area 651.4 cm^2). BIGO T contained only one flux chamber, the second one was replaced by the underwater mass spectrometer TETHYS, operated by R. Camilli (Woods Hole Oceanographic Institution). A TV-guided launching system allowed smooth emplacement of the observatories at selected sites on the sea floor. Several hours after the observatories were placed on the sea floor the chambers were slowly driven into the sediment (~30 cm h^{-1}). During this initial time period, the water inside the flux chamber was periodically replaced with ambient bottom water. After the chamber was fully driven into the sediment, the chamber water was again replaced with ambient bottom water to flush out solutes that might have been released from the sediment during chamber insertion. The water volume enclosed by each benthic chamber was variable but typically ranged from 7 to 18 l. To determine benthic solute fluxes, four (M77/1, M77/2) or eight sequential water samples (M92, M107, M136, M137, MSM17/4) were removed periodically with glass syringes (volume of each syringe ~ 46 to 47 ml). The syringes were connected to the chamber using 1 m long Vygon tubes. Prior to deployment, these tubes were filled with distilled water and care was taken to avoid enclosure of air bubbles. An additional syringe water sampler (4 or 8 sequential samples) was used to monitor the ambient bottom water. The sampling ports for ambient bottom water were positioned about 30–60 cm above the sediment-water interface.

For the measurement of the dinitrogen/argon ratio (N_2/Ar), CO_2 and/or dissolved inorganic carbon (DIC) concentrations on cruises M92, M107, M136, M137, and MSM17/4, water samples were pumped into four (M92, M107, MSM17/4) or eight (M136, M137) 750 mm long glass tubes with an internal diameter of 4.6 mm (volume ~12.5 ml) using self-constructed underwater peristaltic pumps. Prior to deployment, each glass tube was filled with distilled water that was completely replaced by the sample without dilution. Four (M92, MSM17/4) or eight tubes (M136, M137, M107) were used to sample each chamber and the ambient bottom water. During all cruises, the incubations at the sea floor were

https://doi.org/10.5194/essd-2020-308
Preprint. Discussion started: 15 April 2021

conducted for time periods of at least 24 h and to up 48 h, defined as the time interval between insertion of the chamber into the sediment and filling of the last syringe . Immediately after retrieval of the observatories, the water samples were transferred to the on-board cool room for further sample processing.

Dissolved O_2 concentration in each chamber and in the ambient bottom water was measured using optodes (Aanderaa Systems; Tengberg et al., 2006). The precision of the sensors was better at lower concentrations (±0.5 µM) than at higher concentrations of 300–500 µM (±1 µM). The effect of salinity on the measured O_2 concentration was corrected internally by the optode using a salinity of 35. O_2 concentrations were cross-calibrated with automated Winkler O_2 measurements in parallel water samples. For the calculation of the total oxygen uptake (TOU), the linear part of the O_2 time series after the start of the chamber incubation was used. In addition to O_2, fluxes of nitrate (NO_3^-), nitrite (NO_2^-), ammonium (NH_4^+), phosphate (PO_4^3), and silicic acid (H_4SiO_4) were measured routinely. During some lander deployments, further biogeochemical parameters such as sulphide (e.g. M92), dissolved organic matter (M136/M137), or trace metals (M136/M137) were measured.

Fluxes of routinely measured solutes were calculated from the linear increase or decrease of concentration versus time and the height of the water in each chamber. Starting with cruises M136 and M137, a logistic function in addition to linear regression was used to capture the occasional sigmoidal temporal trend of solutes.

The landers were also equipped to recover the surface layer of the incubated sediment (~10–15 cm), which serves as a check for sediment disruption during seafloor operations and chamber insertion. The sediment surface for most deployments during the cruises was intact and undisturbed. The sediment was routinely subsampled for geochemical pore water analysis and depending on the specific goals of the cruise for biological analyses (e.g. foraminifera, sulfur bacteria, bacterial metagenomic analyses, and viruses). Details of sampling and processing of water and sediment samples, as well as their geochemical analysis, are presented in the respective cruise reports and specific publications.

As indicated above, in addition to standard flux measurements of the natural system, during Meteor cruise M137 a series of in situ experiments was conducted. During these incubations, NO_3^- and O_2 concentrations inside the benthic chamber were experimentally manipulated (cf. cruise report by

https://doi.org/10.5194/essd-2020-308
Preprint. Discussion started: 15 April 2021

Sommer et al., 2019). During cruises M136 and M137, the BIGO lander was slightly modified to enable trace metal measurements in the benthic chambers and in the bottom water (cooperation with F. Scholz, GEOMAR). To determine gradients of nutrients and trace metals within the benthic boundary layer the BIGO was equipped with an extendable arm (cooperation with F. Scholz, GEOMAR). Subsequent to the placement of the lander on the seafloor the arm unfolded and allowed water sampling in several heights above the seafloor. Water samples were collected in appropriate sampling bags.

4.5.2 Near-surface sediment coring

Undisturbed sediment cores for the biogeochemical analysis of near surface sediment were retrieved using a multiple-corer (MUC) and using push-cores inserted into the sediment retrieved with the BIGO incubation chambers once on deck. The MUC was equipped with 6–8 Perspex liners 60 cm long with an internal diameter of 10 cm. The MUC was lowered into the sediment with a speed of 0.3 m s^{-1} in all deployments. Once on the sea floor, the liners were pushed into the sediment under gravity by a set of lead weights. Penetration ranged from 10 to 50 cm depending on the sediment type. BIGO push-cores had a diameter of 10 cm and recovered around 5–20 cm of sediment. After retrieval, all cores were transferred to an on-board cool room set to the temperature of the bottom and processed immediately. Supernatant bottom water of the MUC cores was sampled and filtered for subsequent analyses. In general, at least one MUC and one BIGO sediment core was taken at the same site, but not necessarily on the same day. Sub-sampling for redox-sensitive parameters (e.g. dissolved Fe, nutrients) was mainly achieved by sectioning the sediment cores inside an argon filled glove bag. The sampling depth resolution increased from 0.5 or 1 cm at the surface to 4 cm at larger depths. Sediment samples were then spun in a refrigerated centrifuge at 4000 G for 20 min to separate the porewater from the particulates. Subsequently, the porewater samples were filtered (0.2 µm cellulose-acetate syringe filters) under argon. In sandy sediments (MSM17/4, M107), rhizone samplers were used to extract porewaters. All BIGO cores were sectioned either under argon or ambient atmosphere. Standard analytes measured in porewater included nutrients, trace metals, total alkalinity, major ions, and dissolved hydrogen sulphide.

https://doi.org/10.5194/essd-2020-308
Preprint. Discussion started: 15 April 2021

4.5.3 Metabolic rates of benthic microorganisms and their role in benthic N-cycling

Denitrification and oxygen respiration rates of benthic microorganisms (i.e. foraminifera) were measured during one cruise to the Peruvian OMZ (M137) and one research trip to the Swedish Gullmar Fjord (Woehle and Roy, 2018; Glock et al., 2019). The rates were calculated from linear steady-state gradients of nitrous oxide or oxygen in glass microcapsules (after Høgslund et al., 2008; Piña-Ochoa et al., 2010; Glock et al., 2019). Abundances of living benthic foraminifera were determined on three cruises to the Peruvian OMZ (Mallon et al., 2012; Glock et al., 2013; Erdem et al., 2020). Total abundances and individual metabolic rates were used to upscale to the total contribution of foraminifers to benthic N-fluxes and nitrate storage (Glock et al., 2013; Glock et al., 2019). On M137, intracellular phosphate storage was also investigated (Glock et al., 2020).

5 Data availability

Data that has been submitted to the World Data Center PANGAEA (https://www.pangaea.org) is freely available and collection DOIs are listed in Table 2. A complete and up to date list of SFB 754 data available on PANGAEA can be obtained by entering 'SFB754' in the search field. Some of the data collected by the project has not been fully processed and thus has not yet been published. We expect this data to be available in the near future and have included references to it in the tables though the DOIs are not yet available.

Data that has been submitted to the database SOCAT (https://www.socat.info) is freely available.

Data that has been submitted to the database MEMENTO (https://memento.geomar.de) is freely available, but access has to be granted.

Data that has been submitted to the NCBI (https://www.ncbi.nlm.nih.gov/) is freely available.

Data and images that are archived on ExoTaxa (https://ecotaxa.obs-vlfr.fr/) are freely available, but access has to be granted.

https://doi.org/10.5194/essd-2020-308
Preprint. Discussion started: 15 April 2021

6 Conclusions

The SFB 754 project was a milestone for the investigation of biogeochemical and physical interactions in the tropical oceans. The extended period of funding granted by the German Research Foundation allowed for the development of a highly interdisciplinary research program that has lead to a wealth of new insights documented in a large number of publications, theses, and presentations. The open access publication of the large number of different data sets collected during the project can be expected to form a lasting legacy well beyond the project itself. We anticipate and look forward to many more publications and projects that will build upon this unique basis.

7 Author contribution

Each of authors wrote subsections of the manuscript and provided data for the tables. GK combined the input and wrote the common sections. HM handled the data submissions to PANGAEA.

8 Competing interests

The authors declare that they have no conflict of interest.

9 Acknowledgements

We thank the Cape Verdean, Chilean, Ecuadorian, Moroccan, Peruvian, and Senegalese authorities for giving the permission to conduct studies in their territorial waters. We gratefully acknowledge the financial support for the “Sonderforschungsbereich 754: Climate-Biogeochemistry Interactions in the Tropical Ocean” by the DFG. The main support for the cruises M91 and MSM18/3 came through the BMBF-funded joint projects SOPRAN I-III (FKZ 03F0462, 03F0611, and 03F0662). Cruise SO243 was mainly supported by the BMBF-funded project SO243 – ASTRA-OMZ (FKZ 03G0243A). Support for cruises ATA_IFMGEOMAR_4, M80/1, MSM18/2, MSM22, M130, and M145 came also through the BMBF-funded joint projects NORDATLANTIK and RACE (FKZ 03F0443B and 03F0729D).

Cruises MSM22 and M105 received further support from the EU-funded project CARBOCHANGE (grant 264879).

References

Altabet, M., Ryabenko, E., Stramma, L., Wallace, D., Frank, M., Grasse, P., and Lavik, G.: An eddy-stimulated hotspot for fixed nitrogen-loss from the Peru oxygen minimum zone, Biogeosciences, 9(12), 4897-4908, https://doi.org/10.5194/bg-9-4897-2012, 2012.

Arévalo-Martínez, D. L., Beyer, M., Krumbholz, M., Piller, I., Kock, A., Steinhoff, T., Körtzinger, A., and Bange, H. W.: A new method for continuous measurements of oceanic and atmospheric N_2O, CO and CO_2: Performance of off-axis integrated cavity output spectroscopy (OA-ICOS) coupled to non-dispersive infrared detection (NDIR), Ocean Sci., 9, 1071–1087, https://doi.org/10.5194/os-9-1071-2013, 2013.

Arévalo-Martínez, D. L., Steinhoff, T., Brandt, P., Körtzinger, A., Lamont, T., Rehder, G., and Bange, H. W.: N_2O emissions from the northern Benguela upwelling system, Geophys. Res. Lett., 46, 3317–3326, https://doi.org/10.1029/2018GL081648, 2019.

Arévalo-Martínez, D. L. and Mehrtens, H. (Eds.): SFB754 underway trace gases data. PANGAEA, Dataset, https://doi.org/10.1594/PANGAEA.926611, 2021.

Baars, O. and Croot, P. L.: Dissolved cobalt speciation and reactivity in the eastern tropical North Atlantic, Mar. Chem., https://doi.org/10.1016/j.marchem.2014.10.006, 2015.

Bach, L. T., Paul, A. J., Boxhammer, T., von der Esch, E., Graco, M., Schulz, K. G., Achterberg, E. P., Aguayo, P., Arístegui, J., Ayón, P., Baños, I., Bernales, A., Boegeholz, A. S., Chavez, F., Chavez, G., Chen, S.-M., Doering, K., Filella, A., Fischer, M., Grasse, P., Haunost, M., Hennke, J., Hernández-Hernández, N., Hopwood, M. J., Igarza, M., Kalter, V., Kittu, L., Kohnert, P., Ledesma, J., Lieberum, C., Lischka, S., Löscher, C., Ludwig, A., Mendoza, U., Meyer, J., Meyer, J., Minutolo, F., Ortiz Cortes, J., Piiparinen, J., Sforna, C., Spilling, K., Sanchez, S., Spisla, C., Sswat, M., Zavala Moreira, M., and Riebesell, U: Factors controlling plankton community production, export flux, and particulate matter

stoichiometry in the coastal upwelling system off Peru, Biogeosciences, 17(19), 4831-4852, https://doi.org/10.5194/bg-17-4831-2020, 2020.

Bange, H. W., Arévalo-Martínez, D. L., de la Paz. M., Farías, L., Kaiser, J., Kock, A., Law, C. S., Rees, A. P., Rehder, G., Tortell, P. D., Upstill-Goddard, R. C., and Wilson, S. T.: A Harmonized Nitrous Oxide (N_2O) Ocean Observation Network for the 21st Century, Front. Mar. Sci., 6, 157, https://doi.org/10.3389/fmars.2019.00157, 2019.

Berx, B., Cunningham, S., von Appen, W.-J., Atamanchuk, D., Brown, P., Fraser, N., Hahn, J., Jochumsen, K., Johnson, C., de Jong, F., Karstensen, J., King, B., Lankhorst, M., Larsen, K. M. H., McDonagh, E., Moritz, M., and Yashayaev, I.: *AtlantOS EU H2020 633211 Deliverable 3.18*: Report on the observational potential of the TMAs, https://doi.org/10.3289/atlantos_d3.18, 2019.

Bittig, H. C., Körtzinger, A., Neill, C., van Ooijen, E., Plant, J. N., Hahn, J., Johnson, K. S., Yang, B. and Emerson, S. R.: Oxygen optode sensors: principle, characterization, calibration, and application in the ocean, Front. Mar. Sci., 4, 429, https://doi.org/10.3389/fmars.2017.00429, 2018.

Browning, T. J., Achterberg, E. P., Rapp, I., Engel, A., Bertrand, E. M., Tagliabue, A., and Moore, C.M.: Nutrient co-limitation at the boundary of an oceanic gyre, Nature, 551(7679), 242-246, https://doi.org/ 10.1038/nature24063, 2017.

Bohlen L., Dale A. W., Sommer S., Mosch T., Hensen C., Noffke A., Scholz F. and Wallmann K.: Benthic nitrogen cycling traversing the Peruvian oxygen minimum zone, Geochim. Cosmochim. Acta 75, 6094–6111, https://doi.org/10.1016/j.gca.2011.08.010, 2011.

Bourbonnais, A., Altabet, M. A., Charoenpong, C. N., Larkum, J., Hu, H., Bange, H. W., and Stramma, L.: N-loss isotope effects in the Peru oxygen minimum zone studied using a mesoscale eddy as a natural tracer experiment, Global Biogeochem. Cy., 29(6), 793-811, https://doi.org/10.1002/2014GB005001, 2015.

Bourbonnais, A., Letscher, R. T., Bange, H. W., Echevin, V., Larkum, J., Mohn, J.,Yoshida, N. and Altabet, M. A.: N2O production and consumption from stable isotopic and concentration data in the Peruvian coastal upwelling system, Global Biogeochem. Cy., 31(4), 678-698, https://doi.org/10.1002/2016GB005567, 2017.

Bullister, J. L. and Weiss, R. F.: Determination of CCl_3F and CCl_2F_2 in seawater and air, Deep-Sea Res., 35(5), 839-853, https://doi.org/10.1016/0198-0149(88)90033-7, 1988.

Callbeck, C., Lavik, G., Stramma, L., Kuypers, M. M. M., and Bristow, L.: Enhanced nitrogen loss by eddy-induced vertical transport in the offshore Peruvian oxygen minimum zone, PLoS ONE, https://doi.org/10.1371/journal.pone.0170059, 2017.

Callbeck, C. M., Lavik, G., Ferdelman, T. G., Fuchs, B., Gruber-Vodicka, H. R., Hach, P. H., Littmann, S., Schoffelen, N. J., Kavelage, T., Thomsen, S., Schunck, H., Löscher, C. R., Schmitz, R. A., and Kuypers, M. M. M.: Oxygen minimum zone 'cryptic sulfur cycling' sustained by offshore transport of key sulfur oxidizing bacteria, Nat. Commu., 9, 1729, https://doi.org/10.1038/s41467-018-04041-x, 2018.

Chever, F., Rouxel, O. J., Croot, P. L., Ponzevera, E., Wuttig, K., and Auro, M.: Total dissolvable and dissolved iron isotopes in the water column of the Peru upwelling regime, Geochim. Cosmochim. Acta, 162, 66–82, https://doi.org/10.1016/j.gca.2015.04.031, 2015.

Croot, P. L., Heller, M. I., and Wuttig, K.: Redox Processes Impacting the Flux of Iron(II) from Shelf Sediments to the OMZ along the Peruvian Shelf, ACS Earth Sp. Chem., https://doi.org/10.1021/acsearthspacechem.8b00203, 2019.

Croot, P. L., Hopwood, M. J., Rapp, I., and Mehrtens, H. (eds.) (2021): SFB754 trace metal concentrations of water samples, PANGAEA, dataset, https://doi.org/10.1594/PANGAEA.928126, 2021.

Czerny, J. M. S., Hauss, H., Löscher, C. R., and Riebesell, U.: Dissolved N:P ratio changes in the eastern tropical North Atlantic: effect on phytoplankton growth and community structure, Mar. Ecol. Prog. Ser., 545, 49-62, https://doi.org/10.3354/meps11600, 2016.

Cutter, G., Andersson, P., Codispoti, L., Croot, P., Francois, R., Lohan, M., Obata, H., and van der Loeff, M. R.: Sampling and Sample-handling Protocols for GEOTRACES Cruises, V2.0, hdl:10013/epic.42722.d001, 2014.

Czeschel, R., Schütte, F., Weller, R. A., and Stramma, L.: Transport, properties, and life cycles of mesoscale eddies in the eastern tropical South Pacific, Ocean Sci., 14, 731-750, https://doi.org/10.5194/os-14-731-2018.

Dale, A. W., Sommer, S., Ryabenko, E., Noffke, A., Bohlen, L., Wallmann, K., Stolpovsky, K., Greinert, J., and Pfannkuche, O.: Benthic nitrogen fluxes and fractionation of nitrate in the Mauritanian oxygen minimum zone (Eastern Tropical North Atlantic), Geochim. Cosmochim. Acta, 134, 234–256, https://doi.org/10.1016/j.gca.2014.02.026, 2014.

Dale, A. W., Sommer, S., Lomnitz, U., Montes, I., Treude, T., Liebetrau, V., Gier, J., Hensen, C., Dengler, M., Stolpovsky, K., Bryant, L. D., and Wallmann, K.: Organic carbon production, mineralisation and preservation on the Peruvian margin, Biogeosciences 12, 1537–1559, https://doi.org/10.5194/bg-12-1537-2015, 2015.

Dale, A. W., Sommer, S., Lomnitz, U., Bourbonnais, A., and Wallmann, K.: Biological nitrate transport in sediments on the Peruvian margin mitigates benthic sulfide emissions and drives pelagic N loss during stagnation events, Deep-Sea Res. Pt. I, 112, 123–136, https://doi.org/10.1016/j.dsr.2016.02.013, 2016.

Dale, A. W., Graco, M., and Wallmann, K.: Strong and dynamic benthic-pelagic coupling and feedbacks in a coastal upwelling system (Peruvian shelf), Front. Mar. Sci., 4(29), https://doi.org/10.3389/fmars.2017.00029, 2017.

Dale, A. W., Bourbonnais, A., Altabet, M., Wallmann, K., and Sommer, S.: Isotopic fingerprints of benthic nitrogen cycling in the Peruvian oxygen minimum zone, Geochim. Cosmochim. Acta, 245, 406–425, https://doi.org/10.1016/j.gca.2018.10.025, 2019.

Dale, A. W. , Paul, M., Clemens, D. , Scholz, F., Schroller-Lomnitz, U., Wallmann, K. , Geilert, S. , Hensen, C. , Plass, A., Liebetrau, V., Grasse, P., and Sommer, S.: Recycling and burial of biogenic silica in an open margin oxygen minimum zone, Global Biogeochemical Cycles, 35(2), e2020GB006583, https://doi.org/10.1029/2020GB006583, 2021.

Dengler, M. and Sommer, S.: Coupled benthic and pelagic oxygen, nutrient and trace metal cycling, ventilation and carbon degradation in the oxygen minimum zone of the Peruvian continental margin (SFB 754): Cruise No. M 136, 11.04. – 03.05.2017 Callao (Peru) – Callao Solute-Flux Peru I. GEOMAR, Kiel, Germany, 43 pp, https://doi.org/10.3289/CR_M136, 2017.

Dengler, M. and Mehrtens, H. (Eds.): SFB754 turbulence measurements (MSS), PANGAEA, Dataset, https://doi.org/10.1594/PANGAEA.926518, 2021.

Desai, D., Schunck, H., Löser, J., and LaRoche, J.: Fragment Recruitment on Metabolic Pathways (FROMP): Comparative metabolic profiling of metagenomes and metatranscriptomes, Bioinformatics, 29, https://doi.org/10.1093/bioinformatics/bts721, 2013.

Ehlert, C., Grasse, P., Mollier-Vogel, E., Böschen, T., Franz, J., Souza, G., Reynolds, B., Stramma, L., and Frank, M.: Factors controlling the silicon isotope distribution in waters and surface sediments of the Peruvian coastal upwelling, Geochim. Cosmochim. Acta, 99, 128-145, https://doi.org/10.1016/j.gca.2012.09.038, 2012.

Engel, A.: Determination of Marine Gel Particles, in: Practical Guidelines for the Analysis of Seawater, edited, CRC Press, 2009.

Engel, A. and Händel, N.: A novel protocol for determining the concentration and composition of sugars in particulate and in high molecular weight dissolved organic matter (HMW-DOM) in seawater, Mar. Chem., 127, 180–191, https://doi.org/10.1016/j.marchem.2011.09.004, 2011.

Engel, A., Borchard, C., Loginova, A. N., Meyer, J., Hauss, H., and Kiko, R.: Effects of varied nitrate and phosphate supply on polysaccharidic and proteinaceous gel particles production during tropical phytoplankton bloom experiments, Biogeoscience, 12, 5647–5665., https://doi.org/10.5194/bg-12-5647-2015, 2015.

Engel, A. and Galgani, L.: The organic sea-surface microlayer in the upwelling region off the coast of Peru and potential implications for air–sea exchange processes, Biogeosciences, 13, 989–1007, https://doi.org/10.5194/bg-13-989-2016, 2016.

Engel, A., Wagner, H., Le Moigne, F. A., and Wilson, S. T.: Particle export fluxes to the oxygen minimum zone of the eastern tropical North Atlantic, Biogeosciences, 14(7), 1825–1838, https://doi.org/10.5194/bg-14-1825-2017, 2017.

Engel, A. and Mehrtens, H. (Eds.): SFB754 Particulate organic matter and pigment analysis, PANGAEA, Dataset, https://doi.org/10.1594/PANGAEA.926612, 2021.

Engel, A., Loginova, A., Maßmig, M., and Mehrtens, H. (Eds.): SFB754 Dissolved Organic Matter, Cell Abundance, Extracellular Enzyme Rates, and Bacterial Production, PANGAEA, Dataset, https://doi.org/10.1594/PANGAEA.926780, 2021.

Erdem, Z., Schönfeld, J., Glock, N., Dengler, M., Mosch, T., Sommer, S., Elger, J., and Eisenhauer, A.: Peruvian sediments as recorders of an evolving hiatus for the last 22 thousand years, Quat. Sci. Rev., 137, 1–14, https://doi.org/10.1016/j.quascirev.2016.01.029, 2016.

Erdem, Z., Schönfeld, J., Rathburn, A. E., Pérez, M.-E., Cardich, J., and Glock, N.: Bottom-water deoxygenation at the Peruvian margin during the last deglaciation recorded by benthic foraminifera, Biogeosciences, 17, 3165–3182, https://doi.org/10.5194/bg-17-3165-2020, 2020.

Firing, E., and Hummon, J. M.: Ship-mounted Acoustic Doppler Current Profilers. In The GO-SHIP Repeat Hydrography Manual: A Collection of Expert Reports and Guidelines. Hood, E.M., C.L. Sabine, and B.M. Sloyan, eds. IOCCP Report Number 14, ICPO Publication Series Number 134. Available online at: http://www.go-ship.org/HydroMan.html, 2010.

Foltz, G. R., Hummels, R., Dengler, M., Perez, R. C., and Araujo, M.: Vertical turbulent cooling of the mixed layer in the Atlantic ITCZ and trade wind regions, J. Geophys. Res., 125(2), e2019JC015529, https://doi.org/10.1029/2019JC015529, 2020.

Franz, J., Krahmann, G., Lavik, G., Grasse, P., Dittmar, T., and Riebesell, U.: Dynamics and stoichiometry of nutrients and phytoplankton in waters influenced by the oxygen minimum zone in the eastern tropical Pacific, Deep Sea Res. Pt. I, 62, 20–31, https://doi.org/10.1016/j.dsr.2011.12.004, 2012a.

Franz, J., Hauss, H., Sommer, U., Dittmar, T., and Riebesell, U.: Production, partitioning and stoichiometry of organic matter under variable nutrient supply during mesocosm experiments in the tropical Pacific and Atlantic Ocean, Biogeosciences, 9(11), 4629–4643, https://doi.org/10.5194/bgd-9-5755-2012, 2012b.

Frey, C., Bange, H. W., Achterberg, E. P., Jayakumar, A., Löscher, C. R., Arevalo-Martinez, D. L., León-Palmero, E., Sun, M., Xie, R. C., Oleynik, S., and Ward, B.: Regulation of nitrous oxide production in low-oxygen waters off the coast of Peru, Biogeosciences, 17, 2263–2287, https://doi.org/10.5194/bg-17-2263-2020, 2020.

Garcia, H. E., Weathers, K., Paver, C. R., Smolyar, I., Boyer, T. P., Locarnini, R. A., Zweng, M. M., Mishonov, A. V., Baranova, O. K., Seidov, D., and Reagan, J. R.: World Ocean Atlas 2018, Volume 3:

Dissolved Oxygen, Apparent Oxygen Utilization, and Oxygen Saturation. A. Mishonov Technical Ed.; NOAA Atlas NESDIS 83, 38 pp., 2018.

Gier, J., Sommer, S., Löscher, C. R., Dale, A. W., Schmitz, R. A., and Treude, T.: Nitrogen fixation in sediments along a depth transect through the Peruvian oxygen minimum zone, Biogeosciences, 13, 4065–4080, https://doi.org/10.5194/bg-13-4065-2016, 2016.

Gier, J., Löscher, C. R., Dale, A. W., Sommer, S., Lomnitz, U., and Treude, T.: Benthic Dinitrogen Fixation traversing the Oxygen Minimum Zone off Mauritania (NW Africa), Front. Mar. Sci. 4(390), https://doi.org/10.3389/fmars.2017.00390, 2017.

Gledhill, M. and Van Den Berg, C. M. G.: Determination of complexation of iron(III) with natural organic complexing ligands in seawater using cathodic stripping voltammetry, Mar. Chem., 47(1), 41–54, https://doi.org/10.1016/0304-4203(94)90012-4, 1994.

Glock, N., Schönfeld, J., Eisenhauer, A., Hensen, C., Mallon, J., and Sommer, S.: The role of benthic foraminifera in the benthic nitrogen cycle of the Peruvian oxygen minimum zone, Biogeosciences, 10, 4767–4783, https://doi.org/10.5194/bg-10-4767-2013, 2013.

Glock, N., Roy, A.-S., Romero, D.,Wein, T.,Weissenbach, J., Revsbech, N. P., Høgslund, S., Clemens, D., Sommer, S., and Dagan, T.: Metabolic preference of nitrate over oxygen as an electron acceptor in foraminifera from the Peruvian oxygen minimum zone, P. Natl. Acad. Sci. USA, 116, 2860–2865, https://doi.org/10.1073/pnas.1813887116, 2019.

Glock, N., Romero, D., Roy, A. S., Woehle, C., Dale, A. W., Schönfeld, J., Wein, T., Weissenbach, J., and Dagan, T.: A hidden sedimentary phosphate pool inside benthic foraminifera from the Peruvian upwelling region might nucleate phosphogenesis, Geochim. Cosmochimi. Acta, 289, 14–32, https://doi.org/10.1016/j.gca.2020.08.002, 2020.

Glock, N. and Mehrtens, H. (Eds.): SFB754 core-top calibrations of paleo-proxies, PANGAEA, Dataset, https://doi.org/10.1594/PANGAEA.927049, 2021.

Gorsky, G., Ohman, M. D., Picheral, M., Gasparini, S., Stemmann, L., Romagnan, J.-B., Cawood, A., Pesant, S., Garcia-Comas, C., and Pregjer, F.: Digital zooplankton image analysis using the ZooScan integrated system, J. Plankt. Res., 32(3), 285–303, https://doi.org/10.1093/plankt/fbp124, 2010.

Grasse, P., Stichel, T., Stumpf, R., Stramma, L., and Frank, M.: The distribution of neodymium isotopes and concentrations in the Eastern Equatorial Pacific: Water mass advection versus particle exchange, Earth Planet. Sci. Lett., 353, 198–207, https://doi.org/10.1016/j.epsl.2012.07.044, 2012.

Grasse, P., Ehlert, C., and Frank, M.: The influence of water mass mixing on the dissolved Si isotope composition in the Eastern Equatorial Pacific, Earth Planet. Sci. Lett., 380, 60–71, https://doi.org/10.1016/j.epsl.2013.07.033, 2013.

Grasse, P., Ryabenko, E., Ehlert, C., Altabet, M. A., and Frank, M.: Silicon and nitrogen cycling in the upwelling area off Peru: A dual isotope approach, Limnol. Oceanogr., 61(5), 1661–1676., https://doi.org/10.1002/lno.10324, 2016.

Grasse, P., Bosse, L., Hathorne, E. C., Böning, P., Pahnke, K., and Frank, M.: Short-term variability of dissolved rare earth elements and neodymium isotopes in the entire water column of the Panama Basin, Earth Planet. Sci. Lett., 475, 242–253, https://doi.org/10.1016/j.epsl.2017.07.022, 2017.

Grasse, P., Hauss, H., and Mehrtens, H. (Eds.): SFB754 stable and radiogenic isotope measurements, PANGAEA, Dataset, https://doi.org/10.1594/PANGAEA.926530, 2021.

Großkopf, T., Mohr, W., Baustian, T., Schunck, H., Gill, D., Kuypers, M. M. M., Lavik, G., Schmitz, R. A., Wallace, D. W. R., and LaRoche, J.: Doubling of marine dinitrogen-fixation rates based on direct measurements, Nature, 488(7411), 361–364, https://doi.org/10.1038/nature11338, 2012.

Hahn, J., Brandt, P., Greatbatch, R. J., Krahmann, G., and Körtzinger, A.: Oxygen variance and meridional oxygen supply in the tropical North East Atlantic oxygen minimum zone, Climate Dynamics, 43, 2999–3024, https://doi.org/10.1007/s00382-014-2065-0, 2014.

Hahn, J., Krahmann, G., and Mehrtens, H. (Eds.): SFB754 moorings 2006-2018, PANGAEA, Dataset, https://doi.org/10.1594/PANGAEA.926545, 2021.

Hansen, H. P. and Koroleff, F.: Determination of nutrients. In: Methods of seawater analysis. Grasshof, K. (ed), 159–228, 1999.

Hathorne, E., Haley, B., Stichel, T., Grasse, P., Zieringer, M., and Frank, M.: Online preconcentration ICP-MS analysis of rare earth elements in seawater, Geochem. Geophy. Geosy., 13(1), https://doi.org/10.1029/2011gc003907, 2012.

Hauss, H., Franz, J. M., and Sommer, U.: Changes in N: P stoichiometry influence taxonomic composition and nutritional quality of phytoplankton in the Peruvian upwelling, J. Sea Res., 73, 74–85, https://doi.org/10.1016/j.seares.2012.06.010, 2012.

Hauss, H., Kiko, R., and Mehrtens, H. (Eds.): SFB754 Multinet Zooplankton Distribution, PANGAEA, Dataset, https://doi.org/10.1594/PANGAEA.926794, 2021a.

Hauss, H., Kiko, R., Löscher, C. R., and Mehrtens, H. (Eds.): SFB754 Nutrient amendment experiments, PANGAEA, Dataset, https://doi.org/10.1594/PANGAEA.927042, 2021b.

Høgslund, S., Revsbech, N. P. Cedhagen, T. Nielsen, L. P., and Gallardo, V. A.: Denitrification, nitrate turn over, and aerobic respiration by benthic foraminiferans in the oxygen minimum zone off Chile, J. Exp. Mar. Biol. Ecol., 359, 85–91, https://doi.org/10.1016/j.jembe.2008.02.015, 2008.

Holmes, R. M., Aminot, A., Kérouel, R., Hooker, B. A., and Peterson, B. J.: A simple and precise method for measuring ammo-nium in marine and freshwater ecosystems, Can. J. Fish. Aquat.Sci., 56, 1801–1808, https://doi.org/10.1139/cjfas-56-10-1801, 1999.

Hoppe, H.-G.: Significance of exoenzymatic activities in the ecology of brackish water: measurements by means of methylumbelliferyl-substrates, Mar. Ecol.-Prog. Ser., 11, 299–308, https://doi.org/10.3354/meps011299, 1983.

Hu, H., Bourbonnais, A., Larkum, J., Bange, H. W., and Altabet, M. A.: Nitrogen cycling in shallow low oxygen coastal waters off Peru from nitrite and nitrate nitrogen and oxygen isotopes, Biogeosciences, 13(5),1453–1468, https://doi.org/10.5194/bg-13-1453-2016, 2016.

Hydes, D. J., Aoyama, M., Aminot, A., Bakker, K., Becker, S., Coverly, S., Daniel, A., Dickson, A. D., Grosso, O., Kerouel, R., van Ooijen, J., Sato, K., Tanhua, T., Woodward, E. M. S., and Zhang, J.Z.: Recommendations for the Determination of Nutrients in Seawater to High Levels of Precision and Inter-Comparability using Continuous Flow Analysers. Hood, E. M., C. L. Sabine, and B. M. Sloyan, eds. IOCCP Report Number 14, ICPO Publication Series Number 134. Available online at: http://www.go-ship.org/HydroMan.html, 2010.

Kalvelage, T., Jensen, M. M., Contreras, S., Revsbech, N. P., Lam, P., Günter, M., LaRoche, J., Lavik, G., and Kuypers, M. M. M.: Oxygen Sensitivity of Anammox and Coupled N-Cycle Processes in Oxygen Minimum Zones, PLoS ONE, 6(12), https://doi.org/10.1371/journal.pone.0029299, 2011.

Kalvelage, T., Lavik, G., Lam, P., Contreras, S., Arteaga, L., Löscher, C., Oschlies, A., Paulmier, A., Stramma, L., and Kuypers, M.: Nitrogen Cycling Driven By Organic Matter Export In The South Pacific Oxygen Minimum Zone, Nature Geosci., 6, 228–234. https://doi.org/10.1038/ngeo1739, 2013.

Kalvelage, T., Lavik, G., Jensen, M. M, Revsbech, N. P., Löscher, C. R., Schunck, H., Desai, D., Hauss, H., Kiko, R., Holtappels, M., LaRoche, J., Schmitz, R. A., Graco, M. I., and Kuypers. M. M. M.: Aerobic microbial respiration in oceanic oxygen minimum zones, PLoS ONE, 10(7), https://doi.org/10.1371/journal.pone.0133526, 2015.

Kawano, T.: Method for Salinity (Conductivity Ratio) Measurement. In The GO-SHIP Repeat Hydrography Manual: A Collection of Expert Reports and Guidelines. Hood, E. M., C. L. Sabine, and B. M. Sloyan, eds. IOCCP Report Number 14, ICPO Publication Series Number 134. Available online at: http://www.go-ship.org/HydroMan.html, 2010.

Kiko, R., Hauss, H., Dengler, M., Sommer, S., and Melzner, F.: The squat lobster Pleuroncodes monodon tolerates anoxic “dead zone” conditions off Peru, Mar. Bio., 162, 1913–1921, https://doi.org/10.1007/s00227-015-2709-6, 2015.

Kiko, R., Hauss, H., Buchholz, F., and Melzner, F.: Ammonium excretion and oxygen respiration of tropical copepods and euphausiids exposed to oxygen minimum zone conditions, Biogeosciences, 13, 2241–2255, https://doi.org/10.5194/bg-13-2241-2016, 2016.

Kiko, R. and Hauss, H.: On the estimation of zooplankton-mediated active fluxes in Oxygen Minimum Zone regions, Front. Mar. Sci., 6, 741, https://doi.org/10.3389/fmars.2019.00741, 2019.

Kiko, R., Brandt, P., Christiansen, S., Faustmann, J., Kriest, I., Rodrigues, E., Schütte, F., and Hauss, H.: Zooplankton-Mediated Fluxes in the Eastern Tropical North Atlantic, Front. Mar. Sci., 7(358), https://doi.org/10.3389/fmars.2020.00358, 2020.

Kiko, R., Hauss, H., and Mehrtens, H. (Eds.): SFB754 Zooplankton and Particle Distribution from UVP5 measurements, PANGAEA, Dataset, https://doi.org/10.1594/PANGAEA.927040, 2021.

Kiko, R., Hauss, H., and Mehrtens, H. (Eds.): SFB754 Zooplankton Respiration and Ammonium Excretion, PANGAEA, Dataset, https://doi.org/10.1594/PANGAEA.927041, 2021.

Kirchman, D., K'nees, E., and Hodson, R.: Leucine incorporation and its potential as a measure of protein synthesis by bacteria in natural aquatic systems, Appl. Environ. Microbiol., 49, 599–607, https://doi.org/10.1128/AEM.49.3.599-607.1985, 1985.

Knauer, G.A., J. H. Martin, and Bruland, K. W.: Fluxes of particulate carbon, nitrogen, and phosphorus in the upper water column of the northeast Pacific, Deep-Sea Res., 26, 97–108, https://doi.org/10.1016/0198-0149(79)90089-X, 1979.

Krahmann, G. and Mehrtens, H. (Eds.): SFB754 CTD data and additional sensors used on the CTDO system, PANGAEA, Dataset, https://doi.org/10.1594/PANGAEA.926065, 2021a.

Krahmann, G. and Mehrtens, H. (Eds.): SFB754 LADCP data, PANGAEA, Dataset, https://doi.org/10.1594/PANGAEA.926065, 2021b.

Krahmann, G. and Mehrtens, H. (Eds.): SFB754 autonomous glider data, PANGAEA, Dataset, https://doi.org/10.1594/PANGAEA.926547, 2021c.

Krahmann, G. and Mehrtens, H. (Eds.): SFB754 SADCP data (velocities and backscatter), PANGAEA, Dataset, https://doi.org/10.1594/PANGAEA.926521, 2021d.

Krahmann, G. and Mehrtens, H. (Eds.): SFB754 UCTD and rapidcast data, PANGAEA, Dataset, https://doi.org/10.1594/PANGAEA.926529, 2021e.

Krahmann, G. and Mehrtens, H. (Eds.): SFB754 Thermosalinograph (TSG) measurements, PANGAEA, Dataset, https://doi.org/10.1594/PANGAEA.926530, 2021f.

Krahmann, G. and Mehrtens, H. (Eds.): SFB754 Deployments of oxygen-sensor equipped ARGO floats, PANGAEA, Dataset, https://doi.org/10.1594/PANGAEA.926544, 2021g.

Kock, A., Arévalo-Martínez, D. L., Löscher, C. R., and Bange, H. W.: Extreme N_2O accumulation in the coastal oxygen minimum zone off Peru, Biogeosciences, 13(3), 827–840, https://doi.org/10.5194/bg-13-827-2016, 2016.

Langdon, C.: Determination of dissolved oxygen in seawater by winkler titration using the amperometric technique. In The GO-SHIP Repeat Hydrography Manual: A Collection of Expert Reports and Guidelines. Hood, E. M., C. L. Sabine, and B. M. Sloyan, eds. IOCCP Report Number 14, ICPO Publication Series Number 134. Available online at: http://www.go-ship.org/HydroMan.html, 2010.

Lehette, P. and Hernández-León, S.: Zooplankton biomass estimated from digitalized images in Antarctic waters: a calibration exercise, J. Geophys. Res., 111(C5), 1–6, https://doi.org/10.1029/2005JC002887, 2006.

Loginova, A. N., Borchard, C., Meyer, J., Hauss, H., Kiko, R., and Engel, A.: Effects of nitrate and phosphate supply on chromophoric and fluorescent dissolved organic matter in the Eastern Tropical North Atlantic: a mesocosm study, Biogeosciences, 12, 6897–6914, https://doi.org/10.5194/bg-12-6897-2015, 2015.

Loginova, A. N., Thomsen, S., and Engel, A.: Chromophoric and fluorescent dissolved organic matter in and above the oxygen minimum zone off Peru, J. Geophys. Res.: Oceans, 121, 7973–7990, https://doi.org/10.1002/2016JC011906, 2016.

Loginova, A. N., Dale, A. W., LeMoigne, F. A. C., Thomsen, S., Sommer, S., Wallmann, K., and Engel, A.: Sediment release of dissolved organic matter to the oxygen minimum zone off Peru, Biogeosciences, 17, 4663–4679, https://doi.org/10.5194/bg-17-4663-2020, 2020.

Lomnitz, U., Sommer, S., Dale, A. W., Löscher, C. R., Noffke, A., Wallmann, K., and Hensen, C.: Benthic phosphorus cycling in the Peruvian oxygen minimum zone, Biogeosciences, 13, 1367–1386, https://doi.org/10.5194/bg-13-1367-2016, 2016.

Löscher, C. R., Kock, A., Könneke, M., LaRoche, J., Bange, H. W., and Schmitz, R. A.: Production of oceanic nitrous oxide by ammonia-oxidizing archaea, Biogeosciences, 9(7), 2419–2429, https://doi.org/10.5194/bg-9-2419-2012, 2012.

Löscher, C. R., Großkopf, T., Desai, F., Gill, D., Schunck, H., Croot, P., Schlosser, C., Neulinger, S., Pinnow, N., Lavik, G., Kuypers, M. M. M., LaRoche, J. and Schmitz-Streit, R.: Facets of diazotrophy in the oxygen minimum zone waters off Peru, ISME J., 1–13, https://doi.org/10.1038/ismej.2014.71, 2014.

Löscher, C. R., Fischer, M. A., Neulinger, S. C., Philippi, M., Fiedler, B., Hauss, H., Körtzinger, A., Karstensen, J., Künzel, S., Schmitz, R. A., Schütte, F., and Singh, A.: Hidden biosphere in an oxygen-depleted Atlantic open ocean eddy reveals future implications of ocean deoxygenation on primary production in the eastern tropical North Atlantic, Biogeosciences, 12, 7467–7482, https://doi.org/10.5194/bg-12-7467-2015, 2015.

Löscher, C. R., Bourbonnais, A., Dekaezemacker, J., Charoenpong, C. N., Altabet, M. A., Bange, H. W., Czeschel, R., Hoffmann, C., and Schmitz, R.: N_2 fixation in eddies of the eastern tropical South Pacific Ocean, Biogeosciences, 13, 2889–2899, https://doi.org/10.5194/bg-13-2889-2016, 2016.

Löscher, C. R. and Mehrtens, H. (Eds.): SFB754 nitrogen and carbon fixation and N-cycle gene abundance, PANGAEA, Dataset, https://doi.org/10.1594/PANGAEA.926781, 2021a.

Löscher, C. R. and Mehrtens, H. (Eds.): SFB754 Microbial Oxygen Consumption and Nitrogen Loss Processes, PANGAEA, Dataset, https://doi.org/10.1594/PANGAEA.926785, 2021b.

Mallon, J., Glock, N., and Schönfeld, J.: The response of benthic foraminifera to low-oxygen conditions of the Peruvian oxygen minimum zone, in: ANOXIA: Evidence for eukaryote survival and paleontological strategies, Cellular Origin, Life in Extreme Habitats and Astrobiology 21, edited by: Altenbach, A. V., Bernhard, J. M., and Seckbach, J., Springer Science+Business Media, 305-321, https://doi.org/10.1007/978-94-007-1896-8_16, 2012.

Martínez-Pérez, C., Mohr, W., Löscher, C. R., Dekaezemacker, J., Littmann, S., Yilmaz, P., Lehnen, N., Fuchs, B., Lavik, G., Schmitz, R., LaRoche, J., and Kuypers, M. M. M.: The small unicellular diazotrophic symbiont, UCYN-A, is a key player in the marine nitrogen cycle, Nat. Microbiol., https://doi.org/10.1038/nmicrobiol.2016.163, 2016.

Maßmig, M., Lüdke, J., Krahmann, G. and Engel, A.: Bacterial degradation activity in the eastern tropical South Pacific oxygen minimum zone, Biogeosciences, 17, 215–230, https://doi.org/10.5194/bg-17-215-2020, 2020.

McIlvin, M. R. and Altabet, M. A.: Chemical conversion of nitrate and nitrite to nitrous oxide for nitrogen and oxygen isotopic analysis in freshwater and seawater, Anal. Chem., 77, 5589–5595, https://doi.org/10.1021/ac050528s, 2005.

McTaggart, K. E., Johnson, G. J., Johnson, M.C., Delahoyde, F. M., and Swift, J. H.: Notes on CTD/O_2 Data Acquisition and Processing Using Seabird Hardware and Software. In The GO-SHIP Repeat Hydrography Manual: A Collection of Expert Reports and Guidelines. Hood, E. M., C. L. Sabine, and B. M. Sloyan, eds. IOCCP Report Number 14, ICPO Publication Series Number 134. Available online at: http://www.go-ship.org/HydroMan.html, 2010.

Meyer, J., Löscher, C. R., Neulinger, S. C., Reichel, A. F., Loginova, A., Borchard, C., Schmitz, R. A., Hauss, H., Kiko, R., and Riebesell, U.: Changing nutrient stoichiometry affects phytoplankton production, DOP accumulation and dinitrogen fixation – a mesocosm experiment in the eastern tropical North Atlantic, Biogeosciences, 13, 781–794, https://doi.org/10.5194/bg-13-781-2016, 2016.

Mohr, W., Grosskopf, T., Wallace, D. W., and LaRoche, J.: Methodological underestimation of oceanic nitrogen fixation rates, PloS One, 5(9), https://doi.org/10.1371/journal.pone.0012583, 2010.

Mollier-Vogel, E., Ryabenko, E., Martinez, P., Wallace, D., Altabet, M. A., and Schneider, R.: Nitrogen isotope gradients off Peru and Ecuador related to upwelling, productivity, nutrient uptake and oxygen deficiency, Deep-Sea Res. Pt. I, 70, 14–25, https://doi.org/10.1016/j.dsr.2012.06.003, 2012.

Montoya, J. P., Voss, M., Kähler, P., and Capone, D. G.: A simple, high-precision, high-sensitivity tracer assay for N2 fixation, Appl. Environ. Microbiol., 62, 986–993, https://doi.org/10.1128/AEM.62.3.986-993.1996, 1996.

Mortlock, R. A. and Froelich, P. N.: A simple method for the rapid determination of biogenic opal in pelagic marine sediments, Deep-Sea Res., Part A, 36, 1415–1426, https://doi.org/10.1016/0198-0149(89)90092-7, 1989.

Mullison, J.: Backscatter Estimation Using Broadband Acoustic Doppler Current Profilers-Updated. In Proceedings of the ASCE Hydraulic Measurements & Experimental Methods Conference, Durham, NH, USA, 1–5, 2017.

Murphy, K. R., Stedmon, C. A., Graeber, D., and Bro, R.: Fluorescence spectroscopy and multi-way techniques. PARAFAC, Anal. Methods, 5, 6557– 6566, https://doi.org/10.1039/c3ay41160e, 2013.

Noffke, A., Hensen, C., Sommer S., Scholz, F., Bohlen, L., Mosch, T., Graco, M., and Wallmann, K.: Benthic iron and phosphorus fluxes across the Peruvian oxygen minimum zone, Limnol. Oceanogr., 57, 851–867, https://doi.org/10.4319/lo.2012.57.3.0851, 2012.

Pfannkuche, O. and Linke, P.: GEOMAR landers as long-term deep-sea observatories, Sea Techno., 44, 50–55, 2003.

Pfannkuche, O., Schneider, R., Frank, M., and Stramma, L.: Climate-biogeochemistry interactions in the tropical ocean of the SE-American oxygen minimum zone – Cruise No. M77 – October 22, 2008 –

February 18, 2009 – Talcahuano (Chile) -Colon (Panama). Meteor-Berichte, M77, 163 pp. DFG-Senatskommission für Ozeanographie, https://doi.org/10.2312/cr_m77, 2011.

Pfannkuche, O.: Climate-Biogeochemistry interactions in the tropical ocean of the NW-African oxygen minimum zone (SFB754) - Cruise No. MSM17/4 – March 10 – April 11, 2011 – Dakar (Senegal) – Las Palmas (Spain). MARIA S. MERIAN-Berichte, MSM17/4, 59 pp., DFG- Senatskommission für Ozeanographie, https://doi.org/10.2312/cr_msm17_4, 2014.

Picheral, M., Guidi, L., Stemmann, L., Karl, D. M., Iddaoud, G., and Gorsky, G.: The Underwater Vision Profiler 5: An advanced Instrument for high spatial resolution studies of particle size spectra and zooplankton, Limnol. Oceanogr.-Meth., 8, 462–473, https://doi.org/10.4319/lom.2010.8.462, 2010.

Picheral, M., Colin, S., and Irisson, J.-O.: EcoTaxa, a tool for the taxonomic classification of images, http://ecotaxa.obs-vlfr.fr, 2017.

Piña-Ochoa, E., Høgslund, S., Geslin, E., Cedhagen, T., Revsbech, N. P., Nielsen, L. P., Schweizer, M., Jorissen, F., Rysgaard, S., and Risgaard-Petersen, N.: Widespread occurence of nitrate storage and denitrification among Foraminifera and Gromiida, P. Natl. Acad. Sci. USA, 107, 1148–1153, https://doi.org/10.1073/pnas.0908440107, 2010.

Plass A., Schlosser C., Sommer S., Dale A. W., Achterberg E. P., Scholz F., and Helmholtz G.: The control of hydrogen sulfide on benthic iron and cadmium fluxes in the oxygen minimum zone off Peru, Biogeosciences 17, 3685–3704, https://doi.org/10.5194/bg-17-3685-2020, 2020.

Prosser, C. L.: Oxygen: respiration and metabolism, in: Comparative Animal Physiology, edited by: Prosser, C. L. and Brown, F. A., Saunders, Philadelphia, 165–211, 1961.

Rapp, I., Schlosser, C., Rusiecka, D., Gledhill, M., and Achterberg, E. P.: Automated preconcentration of Fe, Zn, Cu, Ni, Cd, Pb, Co, and Mn in seawater with analysis using high-resolution sector field inductively-coupled plasma mass spectrometry, Anal. Chim. Acta, 976, 1–13, https://doi.org/10.1016/j.aca.2017.05.008, 2017.

Rapp, I., Schlosser, C., Menzel Barraqueta, J. L., Wenzel, B., Lüdke, J., Scholten, J., Gasser, B., Reichert, P., Gledhill, M., Dengler, M., and Achterberg, E. P.: Controls on redox-sensitive trace metals in the Mauritanian oxygen minimum zone, Biogeosciences, 16, 4157–4182, https://doi.org/10.5194/bg-16-4157-2019, 2019.

Ryabenko, E., Kock, A., Bange, H. W., Altabet, M. A., and Wallace, D. W.: Contrasting biogeochemistry of nitrogen in the Atlantic and Pacific Oxygen Minimum Zones, Biogeosciences, 9(1), 203–215, https://doi.org/10.5194/bg-9-203-2012, 2012.

Sakamoto, C. M., Johnson, K. S., and Coletti, L. J.: Improved algorithm for the computation of nitrate concentrations in seawater using an in situ ultraviolet spectrophotometer, Limnol. Oceanogr.-Meth., 7, 132–143, https://doi.org/10.4319/lom.2009.7.132, 2009.

Sakamoto, C. M., Johnson, K. S., Coletti, L. J., and Jannasch, H. W.: Pressure correction for the computation of nitrate concentrations in seawater using an in situ ultraviolet spectrophotometer, Limnol. Oceanogr.-Meth., 15, 897–902, https://doi.org/10.1002/lom3.10209, 2017.

Salvatteci, R., Field, D., Sifeddine, A., Ortlieb, L., Ferreira, V., Baumgartner, T., Caquineau, S., Velazco, F., Reyss, J.L., Sanchez-Cabeza, J.A., and Gutierrez, D.: Cross-stratigraphies from a seismically active mud lens off Peru indicate horizontal extensions of laminae, missing sequences, and a need for multiple cores for high resolution records, Marine Geology, 357, 72–89, https://doi.org/10.1016/j.margeo.2014.07.008, 2014.

Salvatteci, R., Gutierrez, D., Sifeddine, A., Ortlieb, L., Druffel, E., Boussafir, M., and Schneider, R.: Centennial to millennial-scale changes in oxygenation and productivity in the Eastern Tropical South Pacific during the last 25 000 years, Quat. Sci. Rev., 131, 102–117, https://doi.org/10.1016/j.quascirev.2015.10.044, 2016.

Salvatteci, R., Schneider, R.R., Blanz, T., and Mollier-Vogel, E.: Deglacial to Holocene Ocean Temperatures in the Humboldt Current System as Indicated by Alkenone Paleothermometry, Geophys. Res. Lett., 46, https://doi.org/10.1029/2018gl080634, 2019.

Salvatteci, R, and Mehrtens, H. (Eds.): SFB754 long gravity cores and piston cores, PANGAEA, Dataset, https://doi.org/10.1594/PANGAEA.927043, 2021a.

Salvatteci, R. and Mehrtens, H. (Eds.): SFB754 age models and sedimentation rates of sediment cores, PANGAEA, Dataset, https://doi.org/10.1594/PANGAEA.927046, 2021b.

Salvatteci, R. and Mehrtens, H. (Eds.): SFB754 downcore X-Ray Fluorescence (XRF) measurements on sediment cores, PANGAEA, Dataset, https://doi.org/10.1594/PANGAEA.927047, 2021c.

Salvatteci, R. and Mehrtens, H. (Eds.): SFB754 downcore proxy records, PANGAEA, Dataset, https://doi.org/10.1594/PANGAEA.927048, 2021d.

Schafstall, J., Dengler, M., Brandt, P., and Bange, H.: Tidal-induced mixing and diapycnal nutrient fluxes in the Mauritanian upwelling region, J. Geophys. Res.-Oceans, 115, C10014, https://doi.org/10.1029/2009jc005940, 2010.

Schlosser, C., Streu, P., Frank, M., Lavik, G., Croot, P. L., Dengler, M., and Achterberg, E. P.: H_2S events in the Peruvian oxygen minimum zone facilitate enhanced dissolved Fe concentrations, Sci. Rep., 8(1), 12642, https://doi.org/10.1038/s41598-018-30580-w, 2018.

Scholz, F., Löscher, C. R., Fiskal, A., Sommer, S., Hensen, C., Lomnitz, U., Wuttig, K., Göttlicher, J., Kossel, E., Steininger, R., and Canfield, D. E.: Nitrate-dependent iron oxidation limits iron transport in anoxic ocean regions, Earth Planet. Sci. Lett., https://doi.org/10.1016/j.epsl.2016.09.025, 2016.

Scholz, F., Siebert, C., Dale, A. W., and Frank, M.: Intense molybdenum accumulation in sediments underneath a nitrogenous water column and implications for the reconstruction of paleo-redox conditions based on molybdenum isotopes, Geochim. Cosmochim, Acta, 213, 400–417, https://doi.org/10.1016/j.gca.2017.06.048, 2017.

Schroller-Lomnitz U., Hensen C., Dale A. W., Scholz F., Clemens D., Sommer S., Noffke A., and Wallmann K.: Dissolved benthic phosphate, iron and carbon fluxes in the Mauritanian upwelling system and implications for ongoing deoxygenation, Deep-Sea Res. Pt. I, 143, 70–84, https://doi.org/10.1016/j.dsr.2018.11.008, 2019.

Schunck, H., Lavik, G., Desai, D. K., Großkopf, T., Kalvelage,T., Löscher, C. R., Paulmier, A., Contreras, S., Siegel, H.,Holtappels, M., Rosenstiel, P., Schilhabel, M. B., Graco, M.,Schmitz, R. A., Kuypers, M. M. M., and LaRoche, J.: GiantHydrogen Sulfide Plume in the Oxygen Minimum Zone off Peru Supports Chemolithoautotrophy, PLoS ONE, 8, e68661, https://doi.org/10.1371/journal.pone.0068661, 2013.

Shcherbina, A. Y., Rudnick, D. L., and Talley, L. D.: Ice-draft profiling from bottom-mounted ADCP data, J. Atmos. Ocean. Technol., 22, 1249–1266, https://doi.org/10.1175/jtech1776.1, 2005.

Simon, M. and Azam, F.: Protein content and protein synthesis rates of planktonic marine bacteria, Mar. Ecol.-Prog. Ser., 51, 201–213, https://doi.org/10.3354/MEPS051201, 1989.

Smith, D. C. and Azam, F.: A simple, economical method for measuring bacterial protein synthesis rates in seawater using ^{3}Hleucine, Mar. Microb. Food Web, 6, 107–114, 1992.

Sommer, S., Türk, M., Kriwanek, S., and Pfannkuche, O.: Gas exchange system for extended in situ benthic chamber flux measurements under controlled oxygen conditions: First application—Sea bed methane emission measurements at Captain Arutyunov mud volcano, Limnol. Oceanogr.-Meth., 6, 23–33, https://doi.org/10.4319/lom.2008.6.23, 2008.

Sommer, S., Linke, P., Pfannkuche, O., Schleicher, T., Schneider v. Deimling, J., Reitz, A., Haeckel, M., Flögel, S., and Hensen, C.: Seabed methane emissions and the habitat of frenulate tubeworms on the Captain Arutyunov mud volcano (Gulf of Cadiz), Mar. Ecol. Prog. Ser., 382, 69–86, https://doi.org/10.3354/meps07956, 2009.

Sommer, S., Dengler, M., and Treude, T.: Benthic element cycling, fluxes and transport of solutes across the benthic boundary layer in the Peruvian oxygen minimum zone, (SFB 754) - Cruise No. M92 – January 05 – February 03, 2013 – Callao (Peru) – Callao (Peru). METEOR-Berichte, M92, 55 pp., DFG-Senatskommission für Ozeanographie, https://doi.org/10.2312/cr_m92, 2014.

Sommer, S., Dengler, M., and Treude, T.: Benthic element cycling, fluxes and transport of solutes across the benthic boundary layer in the Mauritanian oxygen minimum zone, (SFB754) – Cruise No. M107 – May 30 – July 03, 2014 – Fortaleza (Brazil) – Las Palmas (Spain). METEOR- Berichte, M107, 54 pp., DFG-Senatskommission für Ozeanographie, https://doi.org/10.2312/cr_m107, 2015.

Sommer, S., Gier, J., Treude, T., Lomnitz, U., Dengler, M., Cardich, and Dale, A. W.: Depletion of oxygen, nitrate and nitrite in the Peruvian oxygen minimum zone cause an imbalance of benthic nitrogen fluxes, Deep-Sea Res. Pt. I, 112, 113–122, https://doi.org/10.1016/j.dsr.2016.03.001, 2016.

Sommer, S., Dengler, M., and Shipboard Scientific Party: Benthic element cycling, fluxes and transport of nutrients and trace metals across the benthic boundary layer in the Peruvian oxygen minimum zone (SFB 754), Cruise No. 137, 06.05. - 29.05.2017, Callao (Peru) – Callao. METEOR-Berichte, M137, 52 pp., https://doi.org/10.2312/cr_m137, 2019.

Sommer, S., Dale, A., Lomnitz, U., and Mehrtens, H. (Eds.): SFB754 Benthic work (BIGO and MUC geochemistry), PANGAEA, Dataset, https://doi.org/10.1594/PANGAEA.927050, 2021.

Stedmon, C. A. and Bro, R.: Characterizing dissolved organic matter fluorescence with parallel factor analysis: a tutorial, Limnol. Oceanogr.-Meth., 6, 572–579, https://doi.org/10.4319/lom.2008.6.572, 2008.

Swift, J. H.: Reference Quality Water Sample Data: Notes on Data Acquisition. In The GO-SHIP Repeat Hydrography Manual: A Collection of Expert Reports and Guidelines. Hood, E.M., C.L. Sabine, and B.M. Sloyan, eds. IOCCP Report Number 14, ICPO Publication Series Number 134. Available online at: http://www.go-ship.org/HydroMan.html, 2010.

Tanhua, T. and Mehrtens, H. (Eds.): SFB754 hydrochemical measurements from water samples, PANGAEA, Dataset, https://doi.org/10.1594/PANGAEA.926609, 2021.

Tengberg, A., Hovdenes, J., Andersson, H. J., Brocandel, O., Diaz, R., Hebert, D., Arnerich, T., Huber, C., Körtzinger, A., Khripounoff, A., Rey, F., Rönning, C., Schimanski, J., Sommer, S., and Stangelmayer, A.: Evaluation of a lifetime-based optode to measure oxygen in aquatic systems, Limnol. Oceanogr.-Meth., 4, 7–17, https://doi.org/10.4319/lom.2006.4.7, 2006.

Thomsen, S., Kanzow, T., Krahmann, G., Greatbatch, R., Dengler, M., and Lavik, G.: The formation of a subsurface anticyclonic eddy in the Peru-Chile Undercurrent and its impact on the near-coastal salinity, oxygen and nutrient distributions, J. Geophys. Res.: Oceans. 121 (1), 476–501, https://doi.org/10.1002/2015JC010878, 2016.

Thurnherr, A. M., Visbeck, M., Firing, E., King, B. A., Hummon, J. M., Krahmann, G., and Huber, B.: A Manual for Acquiring Lowered Doppler Current Profiler Data. In The GO-SHIP Repeat Hydrography Manual: A Collection of Expert Reports and Guidelines. Hood, E. M., C. L. Sabine, and B. M. Sloyan, eds. IOCCP Report Number 14, ICPO Publication Series Number 134. Available online at: http://www.go-ship.org/HydroMan.html, 2010.

Uchida, H., Johnson, G. C., and McTaggart. K. E.: CTD Oxygen Sensor Calibration Procedures. In The GO-SHIP Repeat Hydrography Manual: A Collection of Expert Reports and Guidelines. Hood, E. M., C. L. Sabine, and B. M. Sloyan, eds. IOCCP Report Number 14, ICPO Publication Series Number 134. Available online at: http://www.go-ship.org/HydroMan.html, 2010.

Ullman, D. S. and Hebert, D.: Processing of Underway CTD Data, J. Atmosp. Ocean. Tech., 31(4), 984–998, https://doi.org/10.1175/JTECH-D-13-00200.1, 2014.

van de Flierdt, T. , Pahnke, K. , Amakawa, H. , Andersson, P. , Basak, C. , Coles, B. , Colin, C. , Crocket, K. , Frank, M. , Frank, N. , Goldstein, S. L. , Goswami, V. , Haley, B. A. , Hathorne, E. C. , Hemming, S. R. , Henderson, G. M. , Jeandel, C. , Jones, K. , Kreissig, K. , Lacan, F. , Lambelet, M. , Martin, E. E. , Newkirk, D. R. , Obata, H. , Pena, L. , Piotrowski, A. M. , Pradoux, C. , Scher, H. D. , Schöberg, H. , Singh, S. K. , Stichel, T. , Tazoe, H. , Vance, D. and Yang, J.: GEOTRACES intercalibration of neodymium isotopes and rare earth element concentrations in seawater and suspended particles. Part 1: reproducibility of results for the international intercomparison, Limnol. Oceanogr.-Meth., 10, 234–251, https://doi.org/10.4319/lom.2012.10.234, 2012.

Woehle, C., Roy, A.-S., Glock, N. , Wein, T., Weissenbach, J., Rosenstiel, P., Hiebenthal, C., Michels, J., Schönfeld, J., and Dagan, T.: A novel eukaryotic denitrification pathway in foraminifera, Curr. Biol., 28, 2536–2543, https://doi.org/10.1016/j.cub.2018.06.027, 2018.

Wuttig, K., Heller, M. I., and Croot, P. L.: Pathways of superoxide (O_2-) decay in the Eastern Tropical North Atlantic, Environ. Sci. Technol., https://doi.org/10.1021/es401658t, 2013.

Xie, R. C., Rehkämper, M., Grasse, P., van de Flierdt, T., Frank, M., and Xue, Z.: Isotopic evidence for complex biogeochemical cycling of Cd in the eastern tropical South Pacific, Earth Planet. Sci. Lett., https://doi.org/10.1016/j.epsl.2019.02.001, 2019.

Zellweger, C., Steinbrecher, R., Laurent, O., Lee, H., Kim, S., Emmenegger, L., Steinbacher, M., and Buchmann, B.: Recent advances in measurement techniques for atmospheric carbon monoxide and nitrous oxide observations, Atmos. Meas. Tech. Discuss., 1–28, https://doi.org/10.5194/amt-2019-108, 2019.

Zsolnay, A., Baiger, E., Jimenez, E., Steinweg, B., and Saccomandi, F.: Differentiating with fluorescence spectroscopy the source of dissolved organic matter in soils subjected to drying, Chemosphere, 38, 45–50, https://doi.org/10.1016/S0045-6535(98)00166-0, 1999.